

การพัฒนาวิธีตรวจวัดคาร์บอนไดออกไซด์ด้วยไฟฟ้าคาร์บอนพิมพ์สกรีน
ดัดแปรด้วยวัสดุระดับนาโนเมตร

นางสาวอภาพร จิระศิริโชติ

จุฬาลงกรณ์มหาวิทยาลัย
CHULALONGKORN UNIVERSITY

บทคัดย่อและแฟ้มข้อมูลฉบับเต็มของวิทยานิพนธ์ตั้งแต่ปีการศึกษา 2554 ที่ให้บริการในคลังปัญญาจุฬาฯ (CUIR)
เป็นแฟ้มข้อมูลของนิสิตเจ้าของวิทยานิพนธ์ ที่ส่งผ่านทางบัณฑิตวิทยาลัย

The abstract and full text of theses from the academic year 2011 in Chulalongkorn University Intellectual Repository (CUIR)
are the thesis authors' files submitted through the University Graduate School.

วิทยานิพนธ์นี้เป็นส่วนหนึ่งของการศึกษาตามหลักสูตรปริญญาวิทยาศาสตรมหาบัณฑิต

สาขาวิชาเคมี ภาควิชาเคมี

คณะวิทยาศาสตร์ จุฬาลงกรณ์มหาวิทยาลัย

ปีการศึกษา 2559

ลิขสิทธิ์ของจุฬาลงกรณ์มหาวิทยาลัย

METHOD DEVELOPMENT FOR DETERMINATION OF CARBOFURAN USING
NANOMATERIAL-MODIFIED SCREEN-PRINTED CARBON ELECTRODE

Miss Apapond Jirasirichote



A Thesis Submitted in Partial Fulfillment of the Requirements
for the Degree of Master of Science Program in Chemistry

Department of Chemistry

Faculty of Science

Chulalongkorn University

Academic Year 2016

Copyright of Chulalongkorn University

Thesis Title	METHOD DEVELOPMENT FOR DETERMINATION OF CARBOFURAN USING NANOMATERIAL-MODIFIED SCREEN-PRINTED CARBON ELECTRODE
By	Miss Apapond Jirasirichote
Field of Study	Chemistry
Thesis Advisor	Assistant Professor Suchada Chuanuwatanakul, Ph.D.
Thesis Co-Advisor	Professor Orawon Chailapakul, Ph.D.

Accepted by the Faculty of Science, Chulalongkorn University in Partial Fulfillment of the Requirements for the Master's Degree

.....Dean of the Faculty of Science
(Associate Professor Polkit Sangvanich, Ph.D.)

THESIS COMMITTEE

.....Chairman
(Associate Professor Vudhichai Parasuk, Ph.D.)

.....Thesis Advisor
(Assistant Professor Suchada Chuanuwatanakul, Ph.D.)

.....Thesis Co-Advisor
(Professor Orawon Chailapakul, Ph.D.)

.....Examiner
(Janjira Panchompoo, Ph.D.)

.....External Examiner
(Assistant Professor Wanida Wonsawat, Ph.D.)

อภาพร จิระศิริโชติ : การพัฒนาวิธีตรวจวัดคาร์โบฟิวแรนโดยใช้ขั้วไฟฟ้าคาร์บอนพิมพ์ สกรีนดัดแปรด้วยวัสดุระดับนาโนเมตร (METHOD DEVELOPMENT FOR DETERMINATION OF CARBOFURAN USING NANOMATERIAL-MODIFIED SCREEN-PRINTED CARBON ELECTRODE) อ.ที่ปรึกษาวิทยานิพนธ์หลัก: ผศ. ดร.สุชาดา จูอนุวัฒน์นกุล, อ.ที่ปรึกษาวิทยานิพนธ์ร่วม: ศ. ดร.อรรวรรณ ชัยลภากุล, 65 หน้า.

งานวิจัยนี้ได้พัฒนาวิธีตรวจวัดคาร์โบฟิวแรนซึ่งเป็นสารฆ่าศัตรูพืชและสัตว์ด้วยเทคนิคไฟฟ้าเพอเรนเซียลพัลส์โวลแทมเมตรีโดยใช้ขั้วไฟฟ้าคาร์บอนพิมพ์สกรีนดัดแปรด้วยแกรฟีนออกไซด์ร่วมกับอนุภาคทองคำระดับนาโนเมตร หากภาวะที่เหมาะสมในการดัดแปรขั้วไฟฟ้า ได้แก่ ปริมาณแกรฟีนออกไซด์ ความเข้มข้นของอนุภาคทองคำระดับนาโนเมตร และพีเอชของสารละลายด้วยการออกแบบการทดลองแบบผสมกลาง ยืนยันเอกลักษณ์ของขั้วไฟฟ้าที่พัฒนาขึ้นด้วยเทคนิคการใช้กล้องจุลทรรศน์อิเล็กตรอนแบบส่องกราดและเอกซเรย์สเปกโทรสโกปีแบบกระจายพลังงาน นอกจากนี้ได้ศึกษาพื้นที่ผิวและกระบวนการทางเคมีไฟฟ้าที่เกิดขึ้นบนขั้วไฟฟ้าดัดแปร ได้ทดลองหาภาวะที่เหมาะสมในการตรวจวัดคาร์โบฟิวแรนด้วยเทคนิคไฟฟ้าเพอเรนเซียลพัลส์โวลแทมเมตรีโดยใช้ขั้วไฟฟ้าคาร์บอนพิมพ์สกรีนดัดแปรด้วยแกรฟีนออกไซด์และอนุภาคทองคำระดับนาโนเมตร ได้แก่ ชนิดของอิเล็กโทรไลต์ ระยะเวลาและศักย์ไฟฟ้าของการสะสม ระยะเวลาและแอมพลิจูดของการกัลวา และการบวนการไฮโดรลิซิสของคาร์โบฟิวแรนไปเป็นคาร์โบฟิวแรน-ฟีนอล ภายใต้ภาวะที่เหมาะสมนี้พบว่า ความสัมพันธ์ระหว่างสัญญาณกับความเข้มข้นของคาร์โบฟิวแรนเป็นเส้นตรงในช่วง 1-30 ไมโครโมลาร์ ($R^2 = 0.9970$) และ 30-250 ไมโครโมลาร์ ($R^2=0.9991$) โดยมีขีดจำกัดต่ำสุดของการตรวจวัดและการหาปริมาณเป็น 0.22 และ 0.72 ไมโครโมลาร์ ตามลำดับ และได้ศึกษาผลการรบกวนการตรวจวัดของสารฆ่าศัตรูพืชและสัตว์อื่น 8 ชนิด นอกจากนี้ ยังสามารถวิเคราะห์ปริมาณคาร์โบฟิวแรนในตัวอย่างแดงกวาและข้าวด้วยวิธีการเติมสารมาตรฐานโดยมีค่าร้อยละการคืนกลับอยู่ในช่วงที่ยอมรับได้ (92.8-107.2%) วิธีตรวจวัดคาร์โบฟิวแรนที่มีสภาพไวและคัดเลือกสูงนี้จึงเป็นวิธีที่ดีสำหรับวิเคราะห์ตัวอย่างทางการเกษตรเนื่องจากทำได้ง่ายและค่าใช้จ่ายไม่แพง

ภาควิชา	เคมี	ลายมือชื่อนิสิต
สาขาวิชา	เคมี	ลายมือชื่อ อ.ที่ปรึกษาหลัก
ปีการศึกษา	2559	ลายมือชื่อ อ.ที่ปรึกษาร่วม

5772221223 : MAJOR CHEMISTRY

KEYWORDS: CARBOFURAN / SCREEN-PRINTED CARBON ELECTRODE / GRAPHENE OXIDE / GOLD NANOPARTICLES

APAPOND JIRASIRICHOTE: METHOD DEVELOPMENT FOR DETERMINATION OF CARBOFURAN USING NANOMATERIAL-MODIFIED SCREEN-PRINTED CARBON ELECTRODE. ADVISOR: ASST. PROF. SUCHADA CHUANUWATANAKUL, Ph.D., CO-ADVISOR: PROF. ORAWON CHAILAPAKUL, Ph.D., 65 pp.

Determination of carbofuran by differential pulse voltammetry using graphene oxide and gold nanoparticles modified screen-printed carbon electrode (AuNPs/GO-SPCE) was developed. The optimization of the amount of graphene oxide, the concentration of gold nanoparticles and pH of supporting electrolyte were conducted by central composite design. The characterization of the developed electrode was carried out by scanning electron microscopy and energy-dispersive X-ray spectroscopy. Moreover, the microscopic electrode surface area and electrochemical behavior of carbofuran were studied by cyclic voltammetry. The operational parameters including type of supporting electrolyte, accumulation time and potential, modulation time and amplitude as well as hydrolysis process of carbofuran to carbofuran-phenol were optimized. Using differential pulse voltammetry on AuNPs/GO-SPCE under optimized conditions, the method exhibited 2 linear ranges of 1-30 ($R^2 = 0.9970$) and 30-250 μM ($R^2=0.9991$) with the limits of detection and quantification of 0.22 and 0.72 μM , respectively. Interfering other effects of eight pesticides were also studied. In addition, application of the proposed method to carbofuran determination in real cucumber and rice samples was achieved by standard addition method with acceptable recoveries of 92.8-107.2%. This sensitive and selective carbofuran detection method is very promising for simple and inexpensive analysis of agricultural samples.

Department: Chemistry

Student's Signature

Field of Study: Chemistry

Advisor's Signature

Academic Year: 2016

Co-Advisor's Signature

ACKNOWLEDGEMENTS

First of all, I would like to thank my advisor, Asst. Prof. Dr. Suchada Chuanuwatanakul and my co-advisor, Prof. Dr. Orawon Chailapakul for training me how to be a scientist, suggestions, guidance and encouragement. I would also like to thank the members of my committee who have helped my work: Dr. Janjira Panchompoo and Assoc. Prof. Dr. Wanida Wonsawat from the Department of Chemistry, Faculty of Science and Technology, Suan Sunandha Rajabhat University, my thesis committee members, for giving valuable comments and advices. I would also like to thank Dr. Eakkasit Punrat and Akkapol Suea-ngam and all the members of the Electrochemistry and Optical Spectroscopy Research Unit for their support, help, and friendship.

The author would like to acknowledge the financial support from Thailand Research Fund through Research Team Promotion Grant (RTA5780005), the Electrochemistry and Optical Research Unit, Department of Chemistry, Faculty of Science, Chulalongkorn University.

Finally, I would like to thank my parents for their love and support during study in the M.Sc. program. My special thanks are extended to everyone who helped me to succeed in this thesis during my time at Chulalongkorn University.

CONTENTS

	Page
THAI ABSTRACT	iv
ENGLISH ABSTRACT	v
ACKNOWLEDGEMENTS	vi
CONTENTS	vii
LIST OF FIGURES	xi
List of Table	xiv
LIST OF ABBREVIATIONS	xv
CHAPTER I INTRODUCTION	1
CHAPTER II THEORETICAL BACKGROUND.....	6
2.1 Electrochemical technique	6
2.1.1 Voltammetry	6
2.1.2. Cyclic voltammetry	7
2.1.3 Differential pulse voltammetry.....	8
2.2 Screen-printed electrochemical sensor	9
2.2.1 Graphene oxide	10
2.2.2 Gold nanoparticles	11
2.3 Central composite design (CCD)	12
2.4 Hydrolysis of carbofuran	14
CHAPTER III EXPERIMENTAL	16
3.1 Instruments and apparatus	16
3.2 Chemicals and reagents.....	17
3.3 Chemicals and reagents preparation	18

	Page
3.3.1 Preparation of 5 μ M of carbofuran-phenol in 0.1 M phosphate buffer (PB) pH 7.4	18
3.3.2 Supporting electrolyte: 0.1 M phosphate buffer pH 7.0.....	18
3.3.3 Supporting electrolyte: 0.1 M acetate buffer	18
3.3.4 Supporting electrolyte: 0.1 M borate buffer.....	19
3.3.5 Supporting electrolyte: 0.1 M Britton-Robinson buffer	19
3.3.6 Synthesis of graphene oxide	19
3.3.7 Synthesis of gold nanoparticles (AuNPs)	19
3.4 Fabrication and modification of electrode.....	20
3.4.1 Screen-printed carbon electrode (SPCE).....	20
3.4.2 Gold nanoparticles and graphene oxide modified screen-printed carbon (AuNPs/GO-SPCE).....	21
3.5 Electrochemical measurements.....	21
3.6 Optimization of the electrode modification parameters	22
3.6.1 Central composite design (CCD) experiments.....	22
3.6.2 Effect of amount of graphene oxide	24
3.6.3 Effect of supporting electrolyte.....	24
3.7 Electrochemical characterization of AuNPs/GOSPCE	24
3.8 Optimization of differential pulse voltammetric (DPV) determination	24
3.9 Hydrolysis of carbofuran	25
3.9.1 Effect of hydrolysis time, temperature and NaOH concentration.....	25
3.10 Analytical performances	25
3.11 Interference study	26
3.12 Analysis of real samples.....	26

	Page
3.13 HPLC measurements.....	27
CHAPTER IV RESULTS AND DISCUSSION	28
4.1 Material and Electrode Characterization.....	28
4.1.1 Characterization of synthesized graphene oxide.....	28
4.1.2 Characterization of synthesized gold nanoparticles.....	29
4.1.3 Surface morphological characterization of electrode	30
4.2 Optimization of electrode modification parameters.....	34
4.2.1 Central composite design (CCD) experiments.....	34
4.3 Electrochemical characterization of AuNPs/GO-SPCE.....	39
4.3.1 Microscopic electrode surface area.....	40
4.3.2 Study of electrochemical process of carbofuran-phenol	41
4.4 Optimization of DPV determination of carbofuran-phenol	43
4.4.1 Effect of the supporting electrolyte	43
4.4.2 Effect of the accumulation time	45
4.4.3 Effect of the accumulation potential.....	46
4.4.4 Effect of the modulation time.....	47
4.4.5 Effect of the modulation amplitude	48
4.5 Hydrolysis of carbofuran	49
4.5.1 Effect of hydrolysis time, temperature and NaOH concentration.....	50
4.6 Analytical performance of DPV determination of carbofuran-phenol.....	52
4.7 Interferences study	53
4.8 Analysis of real samples	55
CHAPTER V CONCLUSIONS.....	57

REFERENCES 60

VITA..... 65



LIST OF FIGURES

		Page
Fig. 2.1	Cyclic voltammetric excitation signal (left) and cyclic voltammogram of a reversible reaction (right).....	8
Fig. 2.2	Waveform (a) and voltammogram of DPV (b) t_p = modulation time, ΔE_p = modulation amplitude.....	9
Fig. 2.3	Structure of graphene oxide (GO).....	10
Fig. 2.4	Interactions between phenolic compounds and graphene oxide.....	11
Fig. 2.5	A Box-Behnken Design for Three Factors.....	12
Fig. 2.6	Hydrolysis of carbofuran (1) and the oxidative reaction equation of carbofuran-phenol (2).....	15
Fig. 3.1	The In-house screen-printed carbon electrodes with three integrated electrodes (WE: carbon working electrode, RE: Ag/AgCl reference electrode and CE: carbon counter electrode).....	20
Fig. 4.1	ATR-FT-IR spectra of graphite and graphene oxide (GO).....	28
Fig. 4.2	UV-vis spectrum of synthesized AuNPs.....	29
Fig. 4.3	Microscopic images of SPCE (a) and AuNPs/GO-SPCE (b) at 20x and 50x (inset).....	30
Fig. 4.4	SEM images of SPCE (a) and AuNPs/GO-SPCE (b) at 1000x and 5000x (inset).....	31
Fig. 4.5	EDX analysis of the surface of SPCE (a) and AuNPs/GO-SPCE (b).....	32
Fig. 4.6	SEM image of AuNPs/GO-SPCE at 5000x (a) and EDX elemental mapping of C, O, Na, S, Cl and Au elements (b).....	33
Fig. 4.7	Typical cyclic voltammograms of 1.0 mM carbofuran-phenol in 0.1 M PB (pH 7.4) on AuNPs/GO-SPCE obtained from the CCD experiments.....	34

- Fig. 4.8** Response surface plots showing the effects of concentration of AuNPs and amount of GO (a), pH of working solution and amount of GO (b), and pH of working solution and concentration of AuNPs (c) on the peak currents of carbofuran-phenol..... 37
- Fig. 4.9** Effect of the amount of GO on the peak current of 1.0 mM carbofuran-phenol in 0.1 M PB (pH 7.4) on AuNPs/GO-SPCE. 38
- Fig. 4.10** Typical cyclic voltammograms of 2.0 mM carbofuran-phenol in 0.1 M PB (pH 7.4) on a SPCE (dotted line), a AuNPs-SPCE (dashed line), a GO-SPCE (dash-dotted line), and a AuNPs/GO-SPCE (solid line)..... 39
- Fig. 4.11** Typical cyclic voltammograms (left) and $I_p-V^{1/2}$ plots of 1.0 mM $[\text{Fe}(\text{CN})_6]^{3-/4-}$ solution containing 0.1 M KCl on a bare SPCE (a) and a AuNPs/GO-SPCE (b) at various scan rates from 20 to 100 mV s^{-1} 41
- Fig. 4.12** Typical cyclic voltammograms (a), $I_p-V^{1/2}$ plot (b), and $\log I_p-\log V$ plot (c) of 2.0 mM carbofuran-phenol in 0.1 M PB (pH 7.4) on AuNPs/GO-SPCE at various scan rates..... 42
- Fig. 4.13** Voltammograms of 0.1 mM carbofuran-phenol in different type of 0.1 M buffer (pH 7.4) using AuNPs/GO-SPCE (a) and plots of peak current versus type of buffer. (b)..... 44
- Fig. 4.14** Effect of the accumulation time on the peak current of 0.1 mM carbofuran-phenol in 0.1 M PB (pH 7.4) using AuNPs/GO-SPCE..... 45
- Fig. 4.15** Effect of the accumulation potential on the peak current of 0.1 mM carbofuran-phenol in 0.1 M PB (pH 7.4) using AuNPs/GO-SPCE..... 46
- Fig. 4.16** Effect of the modulation time on the peak current of 0.1 mM carbofuran-phenol in 0.1 M PB (pH 7.4) using AuNPs/GO-SPCE..... 47
- Fig. 4.17** Effect of the modulation amplitude on the peak current of 0.1 mM carbofuran-phenol in 0.1 M PB (pH 7.4) using AuNPs/GO-SPCE..... 48

- Fig. 4.18** Typical cyclic voltammograms of 2.0 mM carbofuran in 0.1 M PB (pH 7.4), 2.0 mM carbofuran-phenol in 0.1 M PB (pH 7.4), 0.1 M NaOH and blank (0.1 M PB, pH 7.4) on a AuNPs/GO-SPCE..... 49
- Fig. 4.19** Effect of the time and temperature for hydrolysis process on the peak current of hydrolysis product of 0.1 mM carbofuran in PB (pH 7.4) using AuNPs/GO-SPCE. 51
- Fig. 4.20** Typical voltammograms (a) and a standard calibration graph (b) of carbofuran-phenol in 0.1 M PB (pH 7.4) determined by DPV using a AuNPs/GO-SPCE..... 52
- Fig. 4.21** DPV curves of 5 μ M carbofuran-phenol in 0.1 M PB (pH 7.4) on AuNPs/GO-SPCE in the presence of 200 μ M carbendazim (curve a), 5 μ M carbaryl (curve b), 5 μ M propoxur (curve c), 5 μ M isoprocarb (curve d), 5 μ M methiocarb (curve e), or 180 μ M methomyl (curve f). 54
- Fig. 4.22** Standard addition plots for determination of carbofuran in spiked samples of cucumber (a) and rice (b) by the developed method using a AuNPs/GO-SPCE..... 55

List of Table

	Page
Table 2.1	The properties of the three factors of central composite designs..... 13
Table 3.1	List of instruments and apparatus..... 16
Table 3.2	List of chemicals and reagents..... 17
Table 3.3	The actual and code values of each variables..... 22
Table 3.4	Central composite design experiments for optimization of the amount of GO, the concentration of AuNPs and the pH of working solution. 23
Table 4.1	Results of CCD experiments for optimization of the amount of GO, the concentration of AuNPs and the pH of working solution..... 35
Table 4.2	Determination of carbofuran concentration in spiked samples by the developed method using a AuNPs/GO-SPCE and HPLC-UV method..... 56
Table 5.1	Optimization of the DPV parameters for the determination of carbofuran-phenol..... 58

LIST OF ABBREVIATIONS

A	ampere
AuNPs	Gold nanoparticles
AuNPs/GO-SPCE	screen-printed carbon electrode modified GO and AuNPs
CV	cyclic voltammetry
DPV	Differential pulse voltammetry
E	potential
GO	graphene oxide
L	liter
LOD	limit of detection
LOQ	limit of quantification
Mg	milligram
mL	milliliter
mV	millivolt
PVC	polyvinylchloride
RSD	relative standard deviation
SEM	scanning electron microscope
SD	standard deviation
SPCE	screen-printed carbon electrode
V	volt
μg	microgram
μL	microliter
$^{\circ}\text{C}$	degree Celsius

CHAPTER I

INTRODUCTION

In 2015, the population in Thailand was estimated at 68.1 million persons, covered labour force 38.55 million persons. Thirty-two percent of the total labour force was in agricultural sector (12.27 million persons) [1]. The total area of the country was approximately 513,000 square kilometers. Forty-seven percent of the total land area was used for agricultural purposes, thirty-one percent was forest land and twenty-eight percent was unclassified land [2]. According to above mentioned information, Thailand is mostly an agricultural country, not only producing for our consumption but also exporting for benefits. Lately, the agricultural sector has affected Thai economic expansion. In order to obtain higher quality and better yield, farmers used excess pesticides in fruits and vegetables. Thai government has been concerned with the high toxicity of pesticide residues because it is harmful to human health, environment, and international trade. Therefore, determination of pesticide residues in agricultural sector before exportation is required. Recently, rice and other crops were found to be contaminated with pesticides at high level [3]. One of these pesticides is carbofuran.

Carbofuran is one of the most toxic carbamate pesticides. Its commercial names are Furadan, Carbodan, Carbosip, Chinofur, Curaterr, Furacarb, Kenafuran, Pillarfuron, Rampart, Nex, Bay 70143, D 1221, ENT 27164, Yaltox, etc. It was classified as a hazardous substance for human because it damages acetylcholinesterase which is a necessary enzyme of central nerve system. Due to cheapness and high effectiveness of carbofuran, it could be obviously found in field crops including potatoes, corns, soybeans, grapes, soybeans, and wheat [4-7].

After carbofuran was used to control insect in the field crops, the roots of the plants can adsorb carbofuran from the soil and translocate to their organs. The metabolism of carbofuran in plants takes around 30 days to convert to non-toxic compound. Moreover, carbofuran in soil is degraded by chemical hydrolysis and microbial process according to soil pH, clay content, temperature, moisture and microbial population for 26–378 days [8].

Although carbofuran is currently banned in Canada and the European Union, it is still widely used in many countries such as Thailand, China, and India. Therefore, the detection of carbofuran is crucial for both consumer health and environment [9, 10].

Owing to high toxicity, carbofuran detection has been developed by several analytical techniques including gas chromatography [11], high-performance liquid chromatography [12], capillary electrophoresis [13], and mass spectrometry [14]. However, these methods require bulky instruments and leave the large carbon footprint due to a lot of solvent consumption. Thus, the development of electrochemical sensors, which are portable, inexpensive and low consumption of chemicals and samples, has been an active research area for the detection of carbofuran.

Basically, electrochemical sensors for carbofuran detection have been developed to improve the sensitivity and selectivity by coupling with enzymatic materials. For example, in 2011, Sun et al. reported a development of novel gold nanoparticles/L-cysteine/horseradish peroxidase (HRP) on Au for the detection of carbofuran in the concentration range of 0.2-7 μM . The detection limit attained by differential pulse voltammetry (DPV) was 0.18 μM . Recovery values ranging from 98 - 104% were obtained for the analysis of real samples [15].

In 2013, Samphao et al. developed alkaline phosphatase immobilized on a carbon nano-powder paste electrode for the detection of carbofuran by amperometry in the range of 0.05-0.44 μM and LOD equals to 0.05 μM [16].

In 2014, Jeyapragasam et al. reported an electrochemical biosensor based on acetylcholinesterase immobilized onto iron oxide-chitosan nanocomposite for the determination of carbofuran. The linear calibration plot for carbofuran was obtained over the concentration range of 0.005-0.09 μM with a detection limit of 0.0036 μM [17].

However, enzymatic assays are costly as well as require skillful scientist to handle the system. In order to avoid the disadvantages of enzyme-based sensors, there have been reports using electrochemical non-enzymatic sensors such as in 2014, Wang et al. developed a new carbofuran sensor based on the reduced graphene oxide

and cobalt(II) oxide modified on the glassy carbon electrode. The results showed better electrochemical response towards carbofuran. Oxide of metal can increase redox reaction very well. The developed sensor exhibited a linear relationship between DPV response and concentration of carbofuran in the range of 0.2-70 μM . The detection limit was 4.2 $\mu\text{g/L}$. They applied the developed sensor to detect carbofuran in grapes, oranges, tomato, and cabbages [18].

Before detection of carbofuran, non-enzymatic methods require hydrolysis process of carbofuran to carbofuran-phenol for increasing the electrochemical response [19]. On the other hand, phenol derivatives cause electrode fouling after oxidation due to rapid polymerization of electrogenerated phenoxy radicals. The electrochemically generated passive film is strongly adhered on the electrode surface so it needs much of time to clean up [20]. Screen-printed carbon electrode (SPCE) could be an alternative choice due to its disposability with a wide range of potential window, versatility, inexpensiveness and ease of fabrication [21-23]. A new SPCE can be immediately replaced the used one after each measurement [24].

Recently, uses of chemically modified electrodes continuously improve with the great sensitivity of the electrochemical measurements. The outstanding nanomaterials have become interesting materials as the electrode modifiers due to their high surface areas that greatly improve the sensitivity as follow the Cottrell equation [25]. One of nanomaterials that are widely used for electrode modification is gold nanoparticles (AuNPs) which have several benefits such as large effective surface area, good biocompatibility, excellent catalytic property and good electronic property [26, 27]. Furthermore, screen-printed carbon electrodes (SPCEs) modified with gold nanoparticles were characterized by electrochemical impedance spectroscopy (EIS). The data showed an increase in the magnitude of the charge transfer resistance and a decrease of capacitance indicating a partially blocked surface with gold nanoparticles which hinder the electron transfer [28].

Graphene oxide (GO), a well-known two-dimensional (2D) carbon material with hydroxyl and carbonyl functional groups, is also used as an electrode modifier in order to increase the electrochemical sensitivity due to its high adsorption ability and large

surface areas [29]. For example, in 2014, Wong et al. reported the preparation, characterization, and electrochemical behavior of hemin-graphene oxide/glassy carbon electrode for carbofuran detection [30].

The combination of both graphene oxide and gold nanoparticles will be promising materials for carbofuran detection.

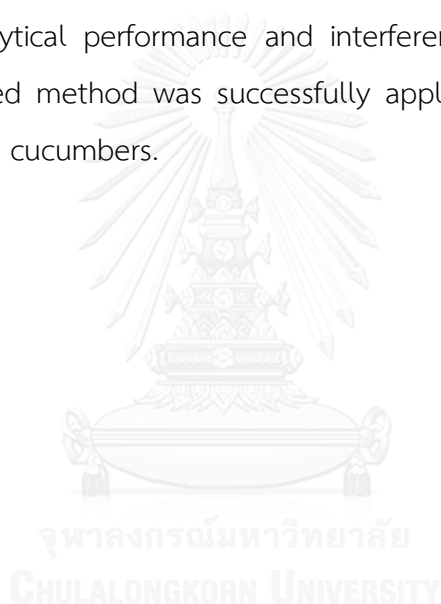
In addition, to optimize the conditions of this proposed method, we used an experimental design called the central composite design (CCD) for optimization of several variables with minimum number of experiments [31, 32]. It allows the ability to consider not only a linear relationship, but also a quadratic relationship when one of variables increases or decreases. Most of researchers perform optimization process with one factor at a time. It means that first parameter is fixed and then second parameter is varied. After that, second parameter is fixed at previous optimized value and then go back to vary the first parameter. This method is exactly correct when two parameters do not have any interaction. Unless they have, the obtained values would be the real optimization. Conversely, CCD can conduct to obtain optimized values whether they interact each other or not. The responses can be carried out to figure out the optimum point of the system [33].

Objectives

- 1) To develop electrochemical sensor based on graphene oxide and gold nanoparticles modified screen-printed carbon electrode.
- 2) To develop determination method for carbofuran using the developed electrochemical sensor.
- 3) To apply the proposed method for carbofuran determination in agricultural products with good accuracy and low detection limits.

Scope of research

In this research, an electrochemical sensor based on a SPCE modified with GO and AuNPs was used to determine carbofuran-phenol. Three analytical conditions including amount of GO, concentration of AuNPs and pH of buffer were optimized by CCD. Effect of pH was selected to study because it disrupts the negative charge on citrate, which acts as a reducing agent and a capping agent in AuNPs synthesis, resulting in aggregation and then decreasing stability of AuNPs [34]. Furthermore, optimization of DPV parameters including supporting electrolyte, the accumulation time, the accumulation potential, the modulation time and the modulation amplitude, effect of hydrolysis time, analytical performance and interference study were investigated. Finally, the developed method was successfully applied for the determination of carbofuran in rice and cucumbers.



CHAPTER II

THEORETICAL BACKGROUND

This chapter consists of the definitions and theoretical electrochemistry which are used in this research. The modification of the working electrode with graphene oxide and gold nanoparticles is defined. Moreover, the hydrolysis of carbofuran pesticide in a basic condition is described.

2.1 Electrochemical technique

The electrochemical techniques provide information on the processes taking place when an electrical potential is applied to the system. Electrochemistry can be used to study the loss of electrons (oxidation) or gain of electrons (reduction) that a substance undergoes during the electrical stimulation. These reduction and oxidation reactions are commonly known as redox reactions and can give information about the concentration, kinetics, reaction mechanisms, chemical status and other behavior of a species in solution. Generally, there are two kinds of electrochemical cells which are galvanic cell and electrolytic cell. Galvanic cell produces an electrical current from energy released by a spontaneous redox reaction while electrolytic cell requires an external source of electrical energy to induce a chemical reaction. Electrolytic method have many advantages, for instance, high sensitivity with a wide linear dynamic range of concentration for both inorganic and organic species, simplicity and rapid analysis time. The selection of the electrochemical techniques depends on the nature of ions or compounds of interest and its interferences in surrounding environment. The following details in this section will focus on the electrochemical techniques that were used in this work.

2.1.1 Voltammetry

Voltammetry is an electrochemical technique which is based on the application of a potential to an electrode surrounded with an electrolyte containing

electroactive species and measuring the signal as a current flowing through that electrode. Voltammetric electrochemical cell is composed of three electrodes which are working electrode (WE), counter electrode (CE) and reference electrode (RE). Working electrode is the most important electrode of electrochemical cell because the interested reaction will happen at the surface of this electrode. Next, counter electrode or auxiliary electrode is an electrode where other reactions or expected reacted reactions occur. Lastly, reference electrode has a stable and well defined electrochemical potential (at constant potential) which the applied or measured potentials in an electrochemical cell are referred.

In this research, voltammetric methods including Cyclic Voltammetry (CV) and Differential Pulse Voltammetry (DPV) were conducted for the carbofuran detection.

2.1.2. Cyclic voltammetry

Cyclic voltammetry (CV) is the most commonly known technique for studying qualitative information of substances, for instance, redox processes, reaction intermediates, and stability of reaction products. Thus, cyclic voltammetry is the first step to perform when electrochemical technique is applied. This technique is based on changing the applied potential of the working electrode in both forward and backward directions at constant scan rate while monitoring the signal current. Electrochemical behavior of the system can be obtained from this simple technique that requires relatively small experimental attempt. Unfortunately, it is difficult to get quantitative information from this technique. Cyclic voltammetry experiment comprises of linear scan potential of a working electrode in an equilibrium unstirred solution by a triangular potential waveform shown in Fig. 2.1. The potential waveform illustrates the forward scan and then backward scan. The measured current at working electrode is plotted versus the applied potential called cyclic voltammogram. Normally, a voltammogram of reversible redox couple during one cycle shows cathodic peak current (i_{pc}) in the forward scan (from positive potential to negative potential) and anodic peak current (i_{pa}) in the reverse scan (from negative potential to

positive potential) at the applied potential approached to the standard potential E° for that redox process. The corresponding peak potential occurring at i_{pc} and i_{pa} named cathodic peak potential (E_{pc}) and anodic peak potential (E_{pa}), respectively.

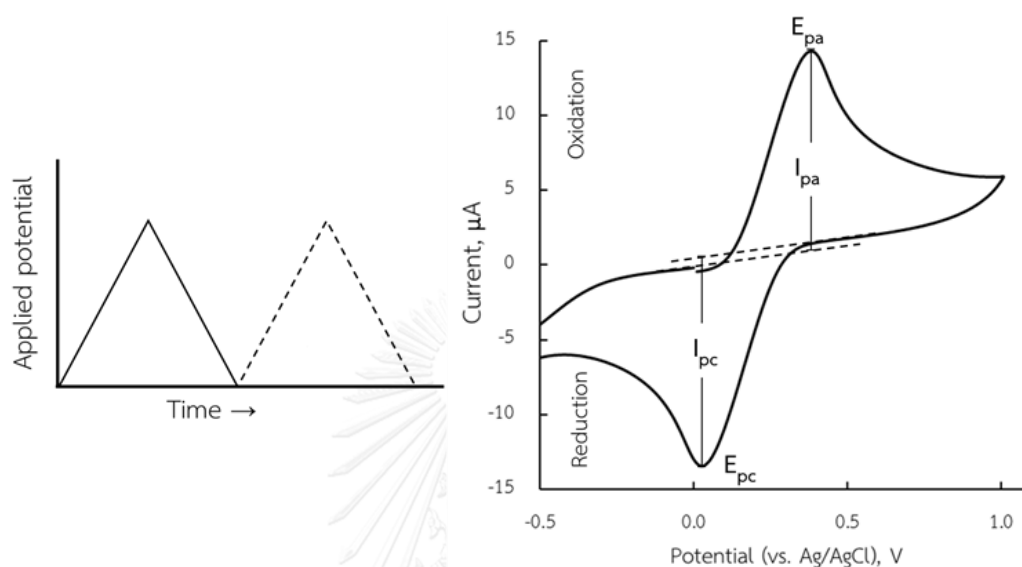


Fig. 2.1 Cyclic voltammetric excitation signal (left) and cyclic voltammogram of a reversible reaction (right) [35].

2.1.3 Differential pulse voltammetry

Differential pulse voltammetry (DPV) is a part of pulse voltammetry. This technique is scanned with a series of pulses. In DPV, potential pulse is fixed and is superimposed on a slowly changing base potential as shown in Fig. 2.2a. The current is measured at two points for each pulse, the first point just before the application of the pulse and the second point at the end of the pulse. These sampling points are selected to allow the decay of the non-faradaic (charging) current. The difference between current measurements at these points for each pulse is determined and plotted against the base potential that are shown in Fig. 2.2b.

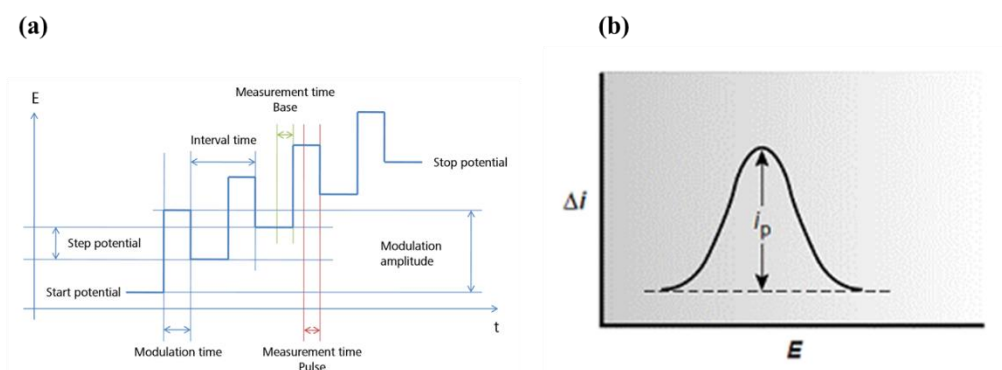


Fig. 2.2 Waveform (a) and voltammogram of DPV (b) [36].

2.2 Screen-printed electrochemical sensor

Screen-printing is a method that has been widely used in artistic applications and more recently in the production of electronic circuits and sensors. Screen-printed sensor consists of silver and carbon ink that is printed through the corresponding mask providing a specific pattern on polyvinyl chloride substrate [29]. Screen-printed electrochemical sensors can be used as whole electrode systems (working, reference and counter electrodes).

The advantages of the screen-printed electrode are ease of fabrication, simplicity, portability, low cost, small size, mass production capabilities and a wide range of designs, which lead to its development in various applications in the electroanalytical field.

2.2.1 Graphene oxide

Graphene oxide (GO) is a unique material that can be viewed as a single monomolecular layer of graphite with various oxygen containing functionalities such as epoxide, carbonyl, carboxyl and hydroxyl groups as shown in Fig. 2.3

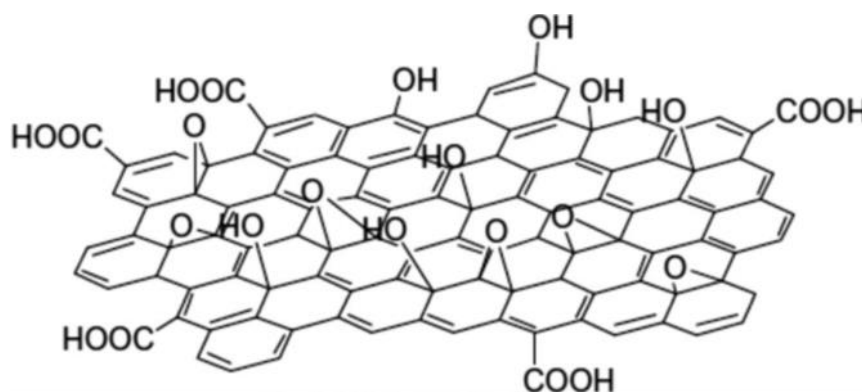


Fig. 2.3 Structure of graphene oxide (GO) [37].

Interest in GO increased dramatically after graphene, a single layer of graphite, was first isolated and studied. GO is stable under both acidic and basic conditions and heat cannot destroy its structure. In addition to being components in electronic devices, GO has been used in nanocomposite materials, polymer composite materials, energy storage, biomedical applications, catalysis, and as a surfactant with some overlaps between these field.

The decorated oxygen groups allowed GO to produce stable dispersion in various non polar and polar solvents such as water which is commonly used as solvent for supporting electrolyte. Moreover, the presence of hydroxyl groups and the oxygen-containing groups could facilitate the interaction between GO and the phenolic compound through π - π interactions and hydrogen bonding as shown in Fig. 2.4. Interestingly, very few reports on the graphene oxide modified on SPCE could be found in electrochemical detecting of phenolic compounds

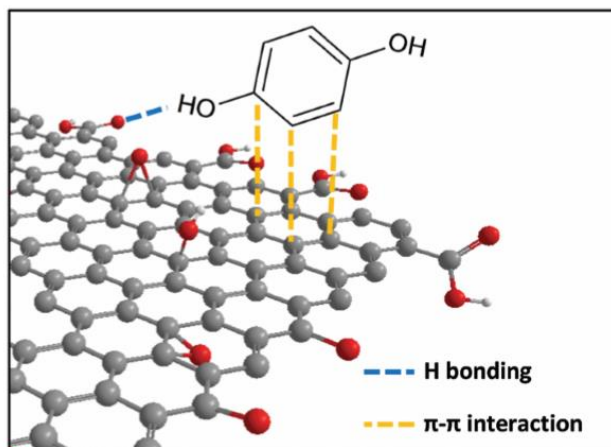


Fig. 2.4 Interactions between phenolic compounds and graphene oxide [38].

2.2.2 Gold nanoparticles

Colloidal gold nanoparticles have been utilized for centuries by artists due to the vibrant colors produced by their interaction with visible light. More recently, these unique optoelectronic properties have been researched and utilized in high technology applications such as organic photovoltaics, sensory probes, therapeutic agents, drug delivery in biological and medical applications, electronic conductors and catalysis. The optical and electronic properties of gold nanoparticles are tunable by changing the size, shape, surface chemistry, or aggregation state.

Gold nanoparticles are used as catalysts in a number of chemical reactions. The surface of gold nanoparticles can be used for selective oxidation. Gold nanoparticles are being developed for sensor. These technologies would be useful in the electrochemical applications.

2.3 Central composite design (CCD)

The term optimization has been used in chemistry for a long time, and for this reason it is a word that always has significance in this branch of the science. The general goal in any optimization is to discover the conditions that produce the best output. This task is usually performed by monitoring the influence of one factor at a time on an experimental response. The main disadvantages of one factor optimization are that it is time consuming and there is a risk of misinterpreting the results if important interactions between factors are present. Central composite design (CCD) is the experimental design which is used to obtain the real optimization.

A Box-Behnken Central Composite Design, commonly called 'a central composite design', contains an imbedded factorial point or fractional factorial design with center point that is augmented with a group of 'axial points' that allow estimation of curvature as shown in Fig. 2.5. Similarly, the number of center point is to contain also depends on certain properties required for the design.

The distance from the center of the design space to a factorial point is ± 1 unit for each factor. Every point can be summarized as in Table 2.1.

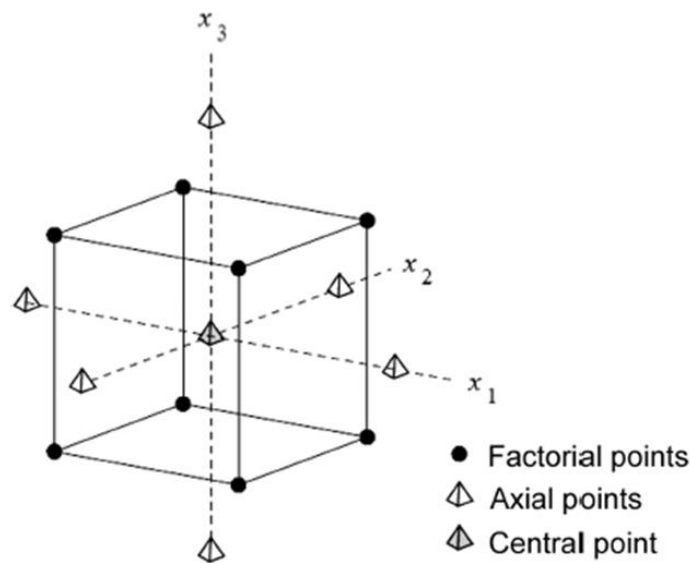


Fig. 2.5 A Box-Behnken Design for Three Factors [39].

Table 2.1 The properties of the three factors of central composite designs.

Run#	X_1	X_2	X_3	Comment
1	1	1	1	Factorial point
2	1	1	-1	Factorial point
3	1	-1	1	Factorial point
4	1	-1	-1	Factorial point
5	-1	1	1	Factorial point
6	-1	1	-1	Factorial point
7	-1	-1	1	Factorial point
8	-1	-1	-1	Factorial point
9	1.68	0	0	Axial point
10	-1.68	0	0	Axial point
11	0	1.68	0	Axial point
12	0	-1.68	0	Axial point
13	0	0	1.68	Axial point
14	0	0	-1.68	Axial point
15	0	0	0	Center point
16	0	0	0	Center point
17	0	0	0	Center point
18	0	0	0	Center point
19	0	0	0	Center point
20	0	0	0	Center point

The experiments were conducted following Table 2.1 and the current can then be obtained. Matrix was used to achieve the coefficient following the equation.

$$b = (D^T * D)^{-1} * D^T * y$$

Finally, multiple linear regression can be obtained from the coefficient which indicates how much the factor impacts on the current.

Predicted data:

$$y' = b_0 + b_1x_1 + b_2x_2 + b_3x_3 + b_4x_1^2 + b_5x_2^2 + b_6x_3^2 + b_7x_1x_2 + b_8x_1x_3 + b_9x_2x_3$$

Therefore, CCD was chosen in the optimization part to find the optimization of amount of GO, concentration of AuNPs and pH of working solution in order to prevent the error and to show whether there is interaction among each other or not.

2.4 Hydrolysis of carbofuran

According to earlier research, Tata and coworker [40] reported that the phenolic derivatives obtained by alkaline hydrolysis oxidize at a relatively lower potential, which increases the sensitivity drastically.

Wei and coworker [19] reviewed that carbofuran with less electrochemical activity could be hydrolyzed in alkaline aqueous solutions at high temperature to form carbofuran-phenol [Fig. 2.6, equation (1)], which showed a good electrochemical response [Fig. 2.6, equation (2)]. Hence carbofuran can be indirectly determined by electrochemically detecting its hydrolysate (carbofuran-phenol).

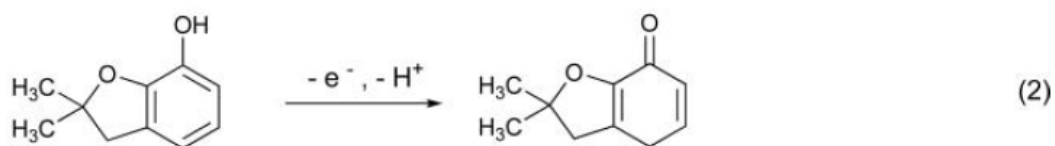
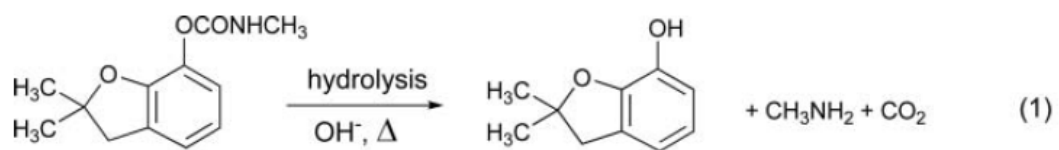


Fig. 2.6 Hydrolysis of carbofuran (1) and the oxidative reaction equation of carbofuran-phenol (2) [19].



CHAPTER III

EXPERIMENTAL

This chapter describes the details of chemicals and materials, instruments and apparatus, solution preparation, synthesis and characterization of graphene oxide (GO) and gold nanoparticles (AuNPs), fabrication and modification of electrodes as well as electrochemical detection and sample preparation method.

3.1 Instruments and apparatus

The instruments and apparatus used in this work are provided in Table 3.1.

Table 3.1 List of instruments and apparatus.

Instruments and apparatus	Suppliers
Autolab PGSTAT30 potentiostat/galvanostat	Metrohm, The Netherlands
Screen-printing blocks	Chaiyaboon, Thailand
Hot air oven	Memmert, USA
Milli-Q water system ($R \geq 18.2 \text{ M}\Omega \text{ cm}^{-1}$)	Millipore, Bedford, USA
Scanning electron microscope (SEM)	JEOL, Japan
FTIR spectrometer Nicolet iS10	Thermo Fisher Scientific, USA
UV-visible spectroscopy	Agilent Technologies, USA
Energy-dispersive X-ray spectrometer (EDX)	JEOL, Japan
Centrifuge (Universal 320R)	Hettich, Germany
Hot plate stirrer, HL HS-115	Harikul Science, Thailand

3.2 Chemicals and reagents

The chemicals and reagents involving in this work were analytical grade. They are listed in Table 3.2.

Table 3.2 List of chemicals and reagents.

Chemicals	Suppliers
2,3-dihydro-2,2-dimethyl-7-benzofuranol (Carbofuran-phenol standard solution)	Sigma-Aldrich
Carbofuran	Sigma-Aldrich
Isoprocarb	Sigma-aldrich
Methiocarb	Sigma-aldrich
Methomyl	Sigma-aldrich
Carbendazim	Sigma-aldrich
Carbayl	Sigma-aldrich
Propoxur	Sigma-aldrich
Chlorpyrifos	Sigma-aldrich
Metalaxyl	Sigma-aldrich
Potassium permanganate (KMnO ₄)	Sigma-aldrich
Sulfuric acid (H ₂ SO ₄)	Merck
Sodium nitrate (NaNO ₃)	Sigma-aldrich
Sodium citrate (C ₆ H ₅ Na ₃ O ₇)	Sigma-aldrich
Chloroauric acid (HAuCl ₄)	Sigma-aldrich
Sodium dihydrogen phosphate (NaH ₂ PO ₄)	Sigma-aldrich
Disodium hydrogen phosphate (Na ₂ HPO ₄)	Sigma-aldrich
Sodium hydroxide (NaOH)	Sigma-aldrich

Chemicals	Suppliers
Sodium tetraborate decahydrate ($\text{Na}_2\text{B}_4\text{O}_7 \cdot 10\text{H}_2\text{O}$)	Sigma-aldrich
Boric acid (H_3BO_3)	Sigma-aldrich
Phosphoric acid (H_3PO_4)	Sigma-aldrich
Acetic acid (CH_3COOH)	Sigma-aldrich
Sodium acetate (CH_3COONa)	Sigma-aldrich
Silver/silver chloride paste	Gwent group
Carbon paste	Gwent group
Graphite powder	Sigma-Aldrich

3.3 Chemicals and reagents preparation

3.3.1 Preparation of 5 μM of carbofuran-phenol in 0.1 M phosphate buffer (PB) pH 7.4

The stock solutions of carbofuran-phenol was prepared by diluting 2,3-dihydro-2,2-dimethyl-7-benzofuranol with 0.10 M PB.

3.3.2 Supporting electrolyte: 0.1 M phosphate buffer pH 7.0

1.4196 g of NaH_2PO_4 was dissolved in 50 mL of Milli-Q water and 0.276 g of Na_2HPO_4 was dissolved in 10 mL of Milli-Q water. Then 40.5 mL of the first solution and 9.5 mL of the second one were mixed together with Milli-Q water to a final volume of 100 mL.

3.3.3 Supporting electrolyte: 0.1 M acetate buffer

2.88 mL of 1 M CH_3COOH and 27.3 mL of 0.3 M CH_3COONa were mixed and filled up to 100 mL with Milli-Q water.

3.3.4 Supporting electrolyte: 0.1 M borate buffer

1.9 g of $\text{Na}_2\text{B}_4\text{O}_7 \cdot 10\text{H}_2\text{O}$ was mixed with 0.04 mL of 6 M HCl and enough Milli-Q water was added to make the total volume up to 100 mL.

3.3.5 Supporting electrolyte: 0.1 M Britton-Robinson buffer

0.23 mL of H_3PO_4 , 0.24 g of H_3BO_3 and 0.23 mL of CH_3COOH were mixed and then 5.7 mL of 0.1 M NaOH was added.

3.3.6 Synthesis of graphene oxide

Graphene oxide (GO) was synthesized following the Hummers' method [41]. Concentrated H_2SO_4 (34.5 mL) was added to a mixture of graphite flakes (1.5 g equivalent weight) and NaNO_3 (0.75 g, 0.5 equivalent weight) and the mixture was cooled to 0°C , then KMnO_4 (4.5 g, 3 equivalent weight) was added in portions. After that, the reaction was adjusted to 35°C and the mixture was stirred for 30 min. Then 69 mL of water was added slowly, producing a large amount of heat that ramped the temperature up to 98°C . Temperature was maintained at 98°C for 15 min and cooled down for 10 min. Additional water (210 mL) and 30% H_2O_2 (1.5 mL) were added. The suspension was dispersed again in Milli-Q water and the mixture was centrifuged (4000 rpm for 1 h), then the solid particles below liquid were kept. The remaining solid material was then washed with 60 mL of water and 60 mL of 30% HCl. The suspension was centrifuged (4000 rpm for 1 h) and the liquid above solid was poured off. The solid obtained was dried at room temperature and 0.6 g of solid remained. Characterization of GO was performed by the attenuated total reflectance Fourier transform infrared spectroscopy (ATR-FTIR).

3.3.7 Synthesis of gold nanoparticles (AuNPs)

Gold nanoparticles were synthesized by Turkevich method [42]. The HAuCl_4 was used as a gold precursor while trisodium citrate was used as a reducing

agent and a stabilizing agent. The method is simple. Briefly, 300 mL of 0.5 M gold(III) chloride solution was put in the beaker and boiled on the hot plate. Then, 30 mL of 38.8 mM trisodium citrate solution was added. Finally, this solution was allowed to cool to room temperature. Characterization of AuNPs were carried out by UV-visible spectroscopy.

3.4 Fabrication and modification of electrode

3.4.1 Screen-printed carbon electrode (SPCE)

First, electrodes were fabricated on PVC sheet. Silver/silver chloride paste was screen-printed onto it to form reference electrodes (RE) and these electrodes were dried in an oven at 55°C for 1 hour. After that, carbon paste was screen-printed onto the same substrate to form working electrodes (WE) as well as counter electrodes (CE). These electrodes are named SPCE (Fig. 3.1).

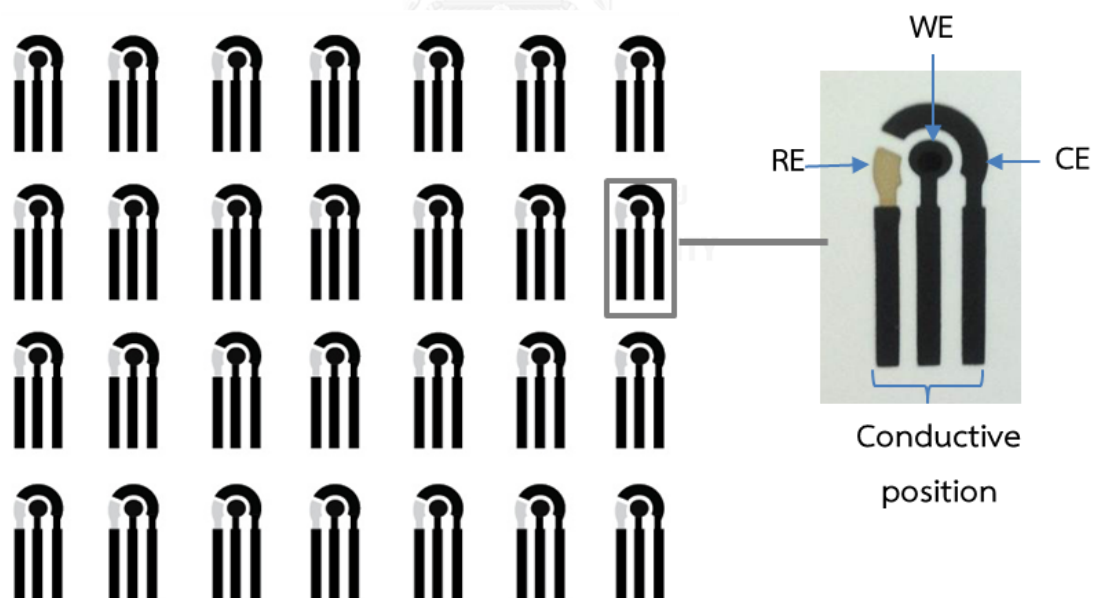


Fig. 3.1 The In-house screen-printed carbon electrodes with three integrated electrodes (WE: carbon working electrode, RE: Ag/AgCl reference electrode and CE: carbon counter electrode).

3.4.2 Gold nanoparticles and graphene oxide modified screen-printed carbon (AuNPs/GO-SPCE)

The electrodes were fabricated via the same process as SPCE. However, a mixture of carbon paste and a suitable amount of GO was used instead of carbon paste. Finally, AuNPs were modified on the working electrodes by drop casting and then the electrodes were allowed to dry at room temperature ($\sim 25^{\circ}\text{C}$). These electrodes are called AuNPs/GO-SPCE.

3.5 Electrochemical measurements

Each electrochemical measurement was carried out by dropping a 100 μL of a working solution onto the surface of in-house AuNPs/GO-SPCE via micropipette. Then, cyclic voltammetry (CV) and differential pulse voltammetry (DPV) were conducted using Autolab PGSTAT30 potentiostat/galvanostat (Metrohm, The Netherlands). All electrochemical experiments were performed at room temperature without purging a working solution with nitrogen gas. DPV was accomplished under the following conditions: step potential 0.01 V, interval time 1 s, modulation time 0.3 s, modulation amplitude 0.15 V, accumulation potential +0.0 V, and accumulation time 60 s.

3.6 Optimization of the electrode modification parameters

3.6.1 Central composite design (CCD) experiments

Important variables affecting the electrochemical performance of AuNPs/GO-SPCE in 1.0 mM carbofuran-phenol solution in 0.1 M PB were optimized by central composite design (CCD). Three considered variables including the amount of GO, the concentration of AuNPs and the pH of working solution were varied within the range of 1.6 to 18.4 mg, 164 to 836 ppm and pH 2 to 12, respectively, while the dependent variable or the response of this method is peak current. The considered variables were assigned as five levels to design 20 experiments. In order to avoid the bias of data analysis, the regression model with the individual variables, interaction and quadratic terms were employed using code values. The actual and code values of all variables are available in Table 3.3. CCD experiments of the five levels are shown in Table 3.4. The predicted responses, the peak currents in this case, were calculated using the obtained regression model to fit the surface response. The suitable conditions that provided the highest predicted response were obtained.

Table 3.3 The actual and code values of each variable

Variables	Code values				
	-1.68	-1	0	1	1.68
Amount of GO (mg)	1.6	5.0	10.0	15.0	18.4
Concentration of AuNPs (ppm)	164	300	500	700	836
pH of working solution	2	4	7	10	12

Table 3.4 Central composite design experiments for optimization of the amount of GO, the concentration of AuNPs and the pH of working solution.

Run#	GO	AuNPs	pH
1	1	1	1
2	1	1	-1
3	1	-1	1
4	1	-1	-1
5	-1	1	1
6	-1	1	-1
7	-1	-1	1
8	-1	-1	-1
9	1.68	0	0
10	-1.68	0	0
11	0	1.68	0
12	0	-1.68	0
13	0	0	1.68
14	0	0	-1.68
15	0	0	0
16	0	0	0
17	0	0	0
18	0	0	0
19	0	0	0
20	0	0	0

3.6.2 Effect of amount of graphene oxide

The effect of the amount of GO on the CV responses of 1.0 mM carbofuran-phenol solution in 0.1 M PB (pH 7.4) was further investigated from 10 mg to 80 mg of GO per 1 g of carbon paste.

3.6.3 Effect of supporting electrolyte

The influence of type of supporting electrolyte on the CV response of 1.0 mM carbofuran-phenol solution was studied in various buffer solution including phosphate buffer, acetate buffer, borate buffer and Britton-Robinson buffer. All supporting electrolytes were fixed at pH 7.4.

3.7 Electrochemical characterization of AuNPs/GOSPCE

To determine the electroactive surface area (A) of the bare SPCE and AuNPs/GO-SPCE. CV of 1.0 mM $\text{Fe}(\text{CN})_6^{3-/4-}$ solution containing 0.1 M KCl at various scan rates (\mathbf{v}) of 20, 40, 60, 80 and 100 mV s^{-1} were conducted. The peak currents were plotted versus the square root of the scan rates ($\mathbf{v}^{1/2}$). Then, the surface area of both electrodes were calculated from Randles-Sevcik equation:

$$I_p = 2.69 \times 10^5 A C n^{3/2} D^{1/2} \mathbf{v}^{1/2}$$

CV was also used to investigate redox process of 1.0 mM carbofuran-phenol in 0.1 M PB (pH 7.4) using AuNPs/GO-SPCE at the scan rates of 20, 40, 60, 80 and 100 mV s^{-1} .

3.8 Optimization of differential pulse voltammetric (DPV) determination

To obtain higher sensitivity, differential pulse voltammetry (DPV) was used to quantify carbofuran. To achieve the optimized detection, DPV parameters were studied including modulation time, modulation amplitude, accumulation potential and accumulation time. The influence of modulation time was investigated in the

range of 0.1 to 0.5 V. After that, the modulation amplitude was varied from 0.01 V to 0.20 V. Finally, the effect of accumulation potential and accumulation time were examined from -0.2 to 0.2 V and 0 to 120 s, respectively.

3.9 Hydrolysis of carbofuran

As previous research, carbofuran with less electrochemical activity can be converted to carbofuran-phenol, which showed a good electrochemical response via hydrolysis process under temperature of 70°C within an hour in basic solution. Comparison of the electrochemical responses of 2.0 mM carbofuran in 0.1 M PB (pH 7.4), 2.0 mM carbofuran-phenol in 0.1 M PB (pH 7.4), 0.1 M NaOH and blank (0.1 M PB, pH 7.4) were conducted by CV.

3.9.1 Effect of hydrolysis time, temperature and NaOH concentration

To obtain higher efficiency with less analysis time, DPV at AuNPs/GO-SPCE was used to optimize hydrolysis time and temperature. First, hydrolysis time of 0.1 mM carbofuran in 0.1 M NaOH at 70°C was investigated in the range of 0 to 60 s. Second, hydrolysis of 0.1 mM carbofuran in 0.1 M NaOH was carried out at various temperature from 25°C to 95°C for 60 s. Finally, the effect of NaOH concentration on alkaline hydrolysis of 0.1 mM carbofuran was compared between 0.1 and 0.5 M.

3.10 Analytical performances

Under the optimized analytical conditions, different concentrations ranging from 1 to 250 μM of carbofuran-phenol in 0.1 M PB solution (pH 7.4) were analyzed by DPV at AuNPs/GO-SPCE. The average peak current for three replicate measurements was plotted versus concentration to obtain the calibration curve where a linear range can be obtained. The limit of detection (LOD) and limit of quantification (LOQ) were achieved from $3\sigma/S$ and $10\sigma/S$, where σ represent the standard deviation of the blank measurements ($n=10$) and S represent the slope of the calibration curve.

3.11 Interference study

To investigate the influence of foreign species on the selectivity of AuNPs/GO-SPCE, separate DPV experiments of other hydrolyzed pesticides, which included chlorpyrifos, metalaxyl, carbendazim, carbaryl, propoxur, isoprocarb, methiocarb and methomyl, were performed. The separate experiments were performed with carbofuran-phenol (5 μM) in 0.1 M electrolyte solution in the presence of 500 μM chlorpyrifos, 500 μM metalaxyl, 200 μM carbendazim, 5 μM carbaryl, 5 μM propoxur, 5 μM isoprocarb, 5 μM methiocarb, or 180 μM methomyl. The tolerance limits are calculated from current interval of carbofuran-phenol within 5%.

3.12 Analysis of real samples

The proposed method was applied to determine carbofuran in samples of cucumbers collected from local market in Nakornpathom province and rice purchased from supermarkets in Bangkok. All samples were prepared as the following procedure.

A 10 g of each sample was spiked with 200 μL of 55.30 mg/L carbofuran standard solution (equivalent to 1.106 mg/kg) or 200 μL of 331.8 mg/L carbofuran standard solution (equivalent to 6.636 mg/kg) and then ground and blended. The sample was exposed to 60 mL chloroform for one day. After this first step, conventional filtration was carried out to remove insoluble substances. The filtrate was then evaporated to dryness and the residue was dissolved in ethanol. Subsequently, 0.1 M sodium hydroxide was added and the solution was heated at a temperature of 70°C for 40 min to hydrolyze the carbofuran to carbofuran-phenol. The resulting solution was neutralized with HClO_4 and diluted to 10 mL with 0.1 M PB (pH 7.4) [30]. Then, the standard addition method was applied to determine carbofuran-phenol in the prepared sample solution. The obtained results were based on triplicate measurements ($n=3$). The percent recovery can be obtained from the following formula:

$$\text{Percent recovery} = \frac{\text{Found concentration of spiked sample}}{\text{Known concentration of spiked sample}} \times 100$$

3.13 HPLC measurements

To validate the proposed method, the results were compared with standard method obtained by HPLC-UV. The HPLC with C18-column (150 mm × 4.6 mm) and UV detector were used to validate the results of the carbofuran detection in real samples. HPLC measurements were performed in triplicate with the following conditions: mobile phase of acetonitrile and water (55:45 v/v), flow rate of 1.0 mL min⁻¹, sample injection volume of 20 µL, and detection wavelength of 280 nm [30].



CHAPTER IV

RESULTS AND DISCUSSION

This chapter presents the results and discussion of the characterization of synthesized GO and AuNPs, characterization of AuNPs/GO-SPCE, optimization of the DPV determination of carbofuran at AuNPs/GO-SPCE, analytical performance and analytical applications.

4.1 Material and Electrode Characterization

4.1.1 Characterization of synthesized graphene oxide

GO was synthesized from graphite powder according to the Hummers' method. Graphite and GO were characterized by ATR FT-IR to investigate the functional group of GO. FT-IR spectrum of graphite shows no significant peak because graphite is made only of carbon atoms. Nevertheless, the synthesized GO shows three characteristic peaks: O-H stretching vibration at 3120.71 cm^{-1} , C=O stretching vibration at 1715.92 cm^{-1} and remaining sp^2 stretching vibration at 1574.43 cm^{-1} as shown in Fig. 4.1. This result confirms that the synthesized material was GO [43].

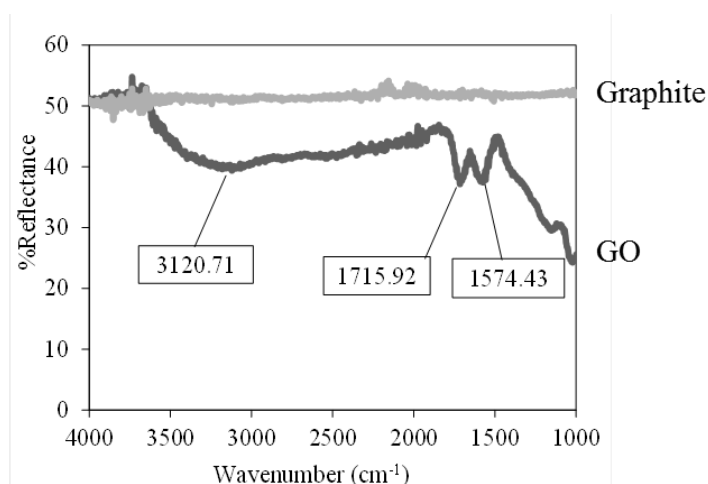


Fig. 4.1 ATR-FT-IR spectra of graphite and graphene oxide (GO).

4.1.2 Characterization of synthesized gold nanoparticles

AuNPs were synthesized by the reduction of HAuCl_4 with trisodium citrate ($\text{Na}_3\text{C}_6\text{H}_5\text{O}_7$) which acted as a reducing agent and stabilizer using Turkevich method. After adding trisodium citrate into the solution of gold(III), the color of the solution slowly turned into red wine indicating of nanoparticles. The plasmonic extinction spectrum of synthesized AuNPs (Fig. 4.2) was obtained by UV-visible spectroscopy. It shows a single band at around 520 nm, which is the characteristic peak of the surface plasmon absorption of AuNPs with a diameter around 20 nm [44].

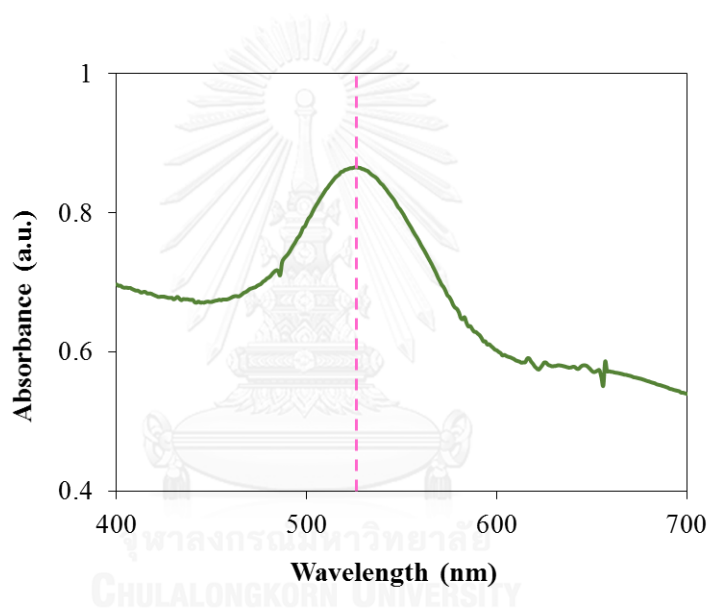


Fig. 4.2 UV-vis spectrum of synthesized AuNPs.

4.1.3 Surface morphological characterization of electrode

Scanning electron microscopy (SEM) and Energy-dispersive X-ray spectroscopy (EDX) were used to investigate the morphology of the electrode. As shown in Fig. 4.3, the surface of bare SPCE (Fig. 4.3 a) was dark while the surface of AuNPs/GO-SPCE (Fig. 4.3 b) was brighter and the color of the AuNPs was uniformly distributed. Consequently, the microscopic images illustrated that the AuNPs was successfully covered the area of AuNPs/GO-SPCE.

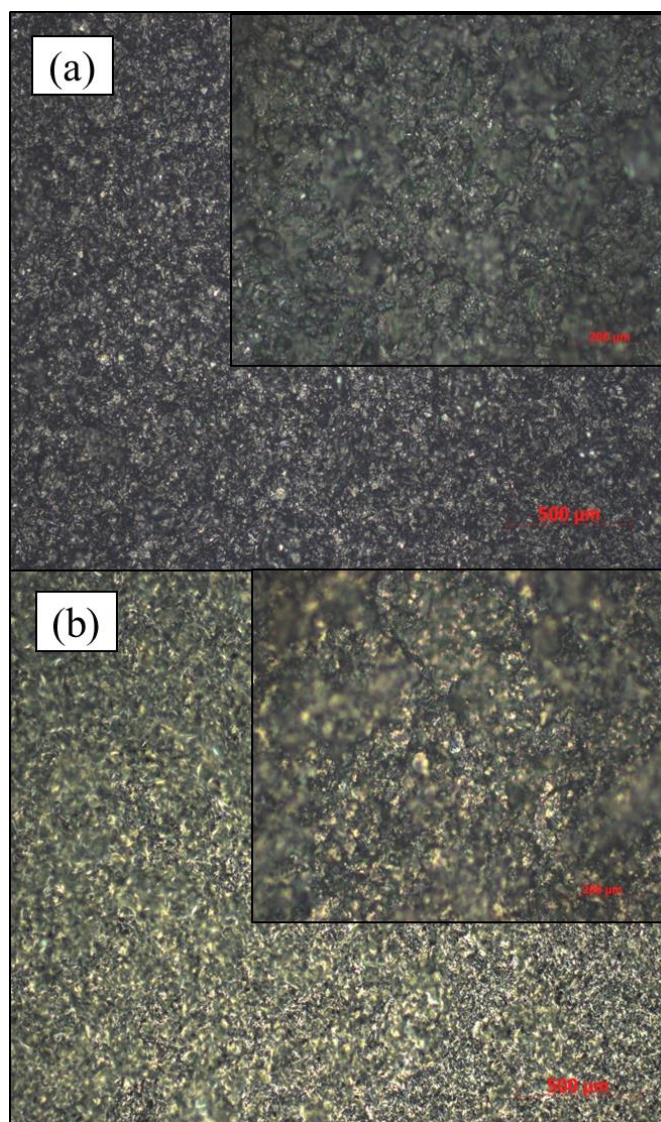


Fig. 4.3 Microscopic images of SPCE (a) and AuNPs/GO-SPCE (b) at 20x and 50x (inset).

The SEM images of SPCE and AuNPs/GO-SPCE are shown in Fig. 4.4. The surface of the bare electrode presented a smooth platelet of carbon (Fig 4.4 a). In the case of the modified electrode, there were numerous linked-small particles covering the whole surface (Fig 4.4 b). It can be concluded that AuNPs were successfully modified on the surface of GO-SPCE.

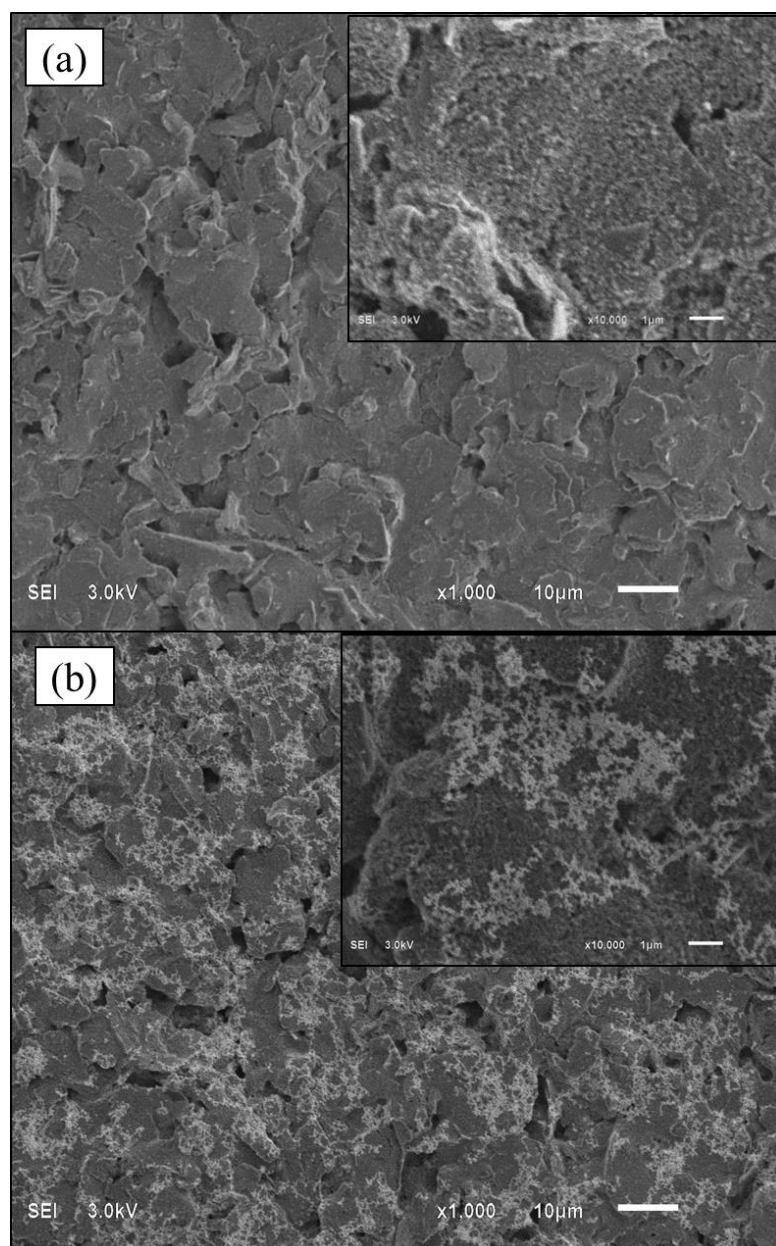


Fig. 4.4 SEM images of SPCE (a) and AuNPs/GO-SPCE (b) at 1000x and 5000x (inset).

Moreover, the elements on the surface of SPCE and AuNPs/GO-SPCE were also investigated by EDX. Fig. 4.5 a and b show the EDX analysis results of SPCE and AuNPs/GO-SPCE, respectively. They revealed that the percentage of O element increased from 0.65% in the bare SPCE to 1.75% in AuNPs/GO-SPCE because of the presence of GO on the electrode. Au element increased from 0% to 7.15% resulting in AuNPs exactly appearing on the electrode.

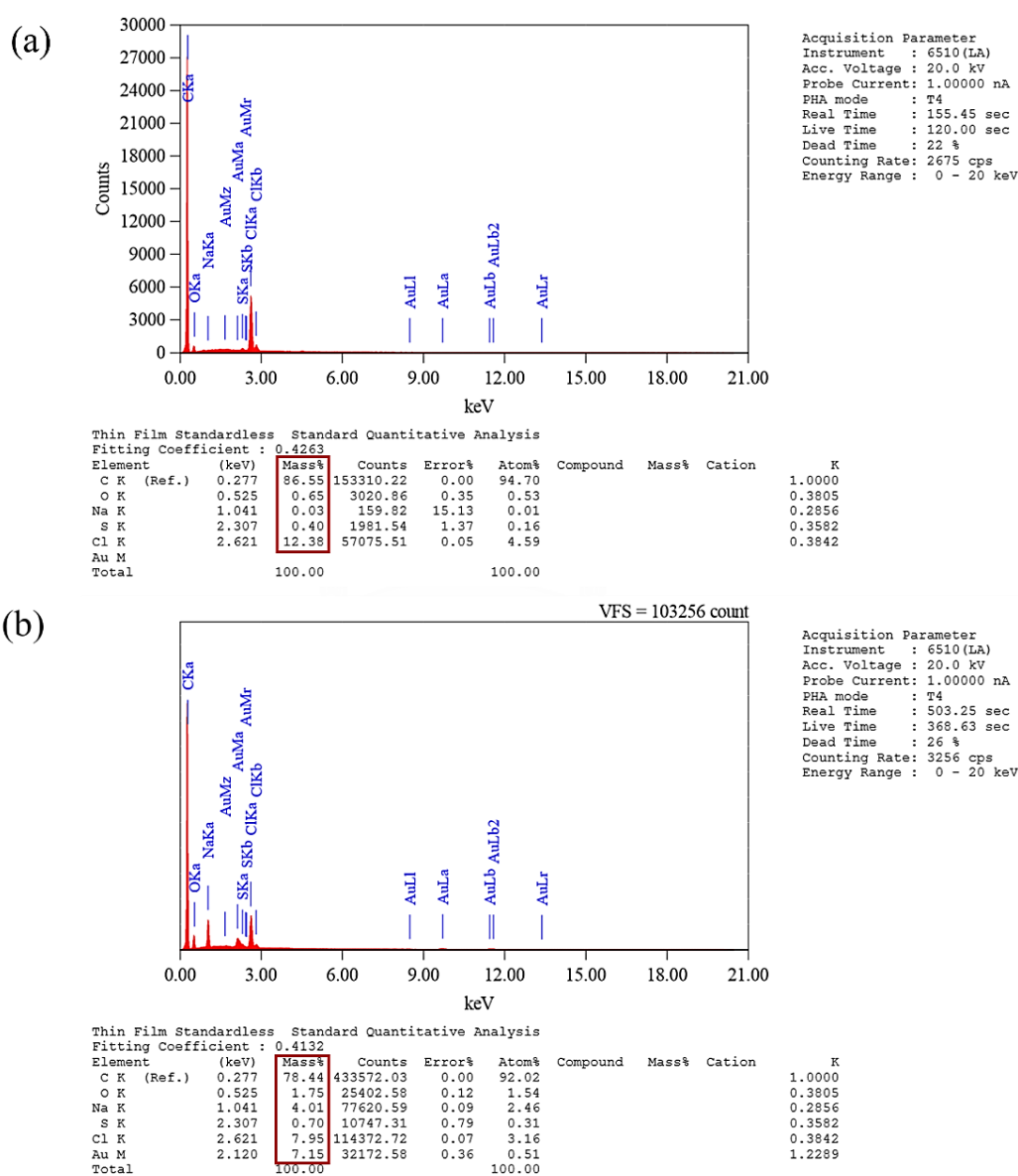


Fig. 4.5 EDX analysis results of the surface of SPCE (a) and AuNPs/GO-SPCE (b).

The EDX mapping images are illustrated in Fig. 4.6. White area in SEM image (Fig. 4.6 a) was Au element indicating the presence of Au on the electrode surface. Na and Cl elements obviously occurred at the same position suggested that there are NaCl impurities on the surface of electrode. However, they did not interfere the electrochemical detection of carbofuran. These results confirmed that the electrode was successfully modified with GO and AuNPs. GO and AuNPs can be used as alternative electrodes modifiers to enhance the electrochemical performance of the sensor.

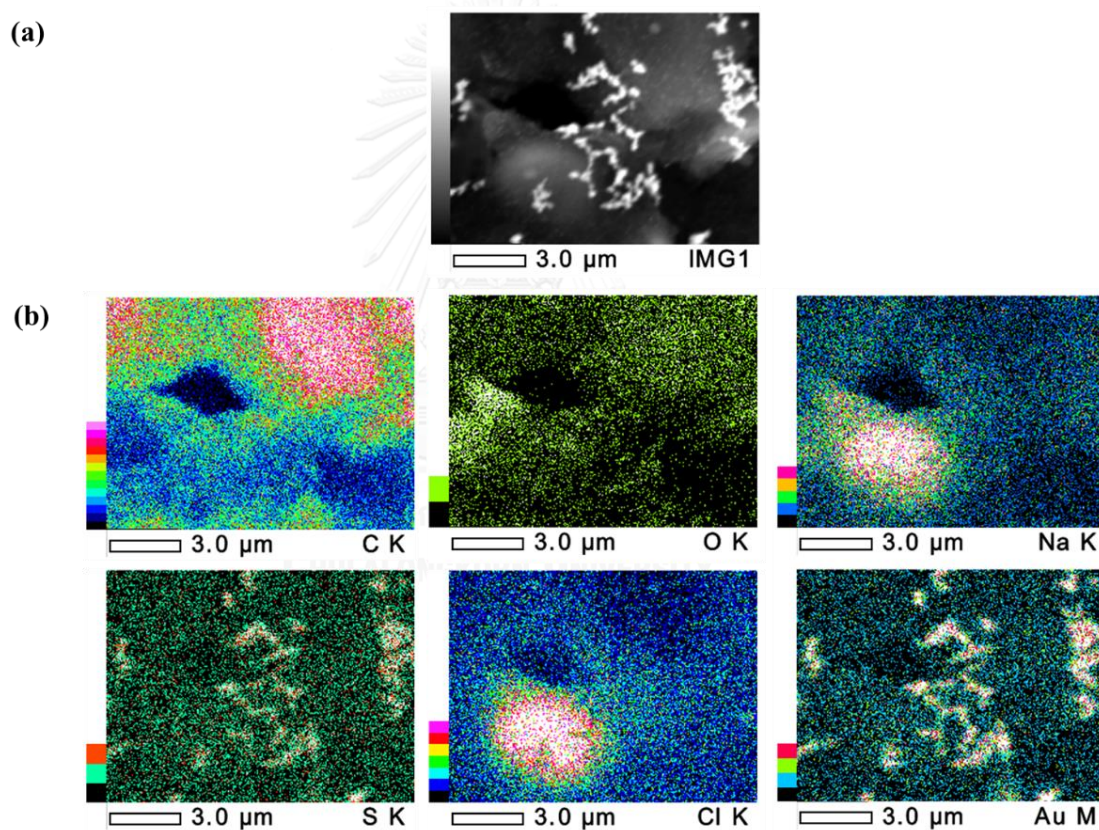


Fig. 4.6 SEM image of AuNPs/GO-SPCE at 5000x (a) and EDX elemental mapping of C, O, Na, S, Cl and Au elements (b).

4.2 Optimization of electrode modification parameters

4.2.1 Central composite design (CCD) experiments

In this research, GO was used as electrode modifier by mixing into the carbon paste before screen-printing onto PVC substrate to form the working and counter electrodes. AuNPs were then modified on the working electrodes by drop casting. Therefore, three electrode modification variables including the amount of GO, the concentration of AuNPs and the pH of working solution were optimized via central composite design (CCD) method.

The amount of GO and the concentration of AuNPs in the solution used to modify electrodes were varied from 1.6 to 18.4 mg and 164 to 836 ppm, respectively. Furthermore, the pH of working solution was varied over the range of 2-12 because pH is the factor that disrupts the negative charge on citrate resulting in aggregation of the nanoparticles and hence decreasing the stability of AuNPs. CVs of 1.0 mM carbofuran-phenol solution in 0.1 M PB at various pH on AuNPs/GO-SPCE with different compositions were obtained as shown in Fig. 4.7 and the resulting peak currents are reported in Table 4.1.

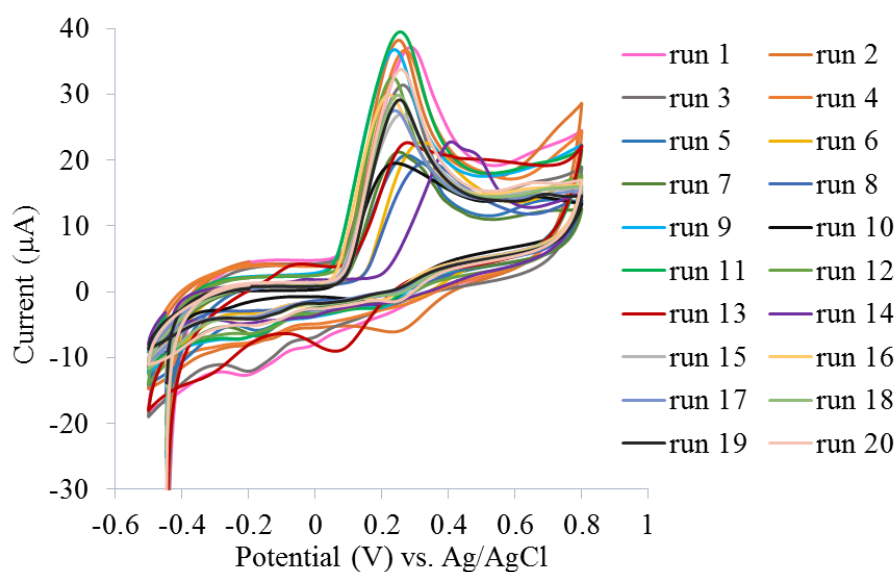


Fig. 4.7 Typical cyclic voltammograms of 1.0 mM carbofuran-phenol in 0.1 M PB (pH 7.4) on AuNPs/GO-SPCE obtained from 20 CCD experiments.

Table 4.1 Results of CCD experiments for optimization of the amount of GO, the concentration of AuNPs and the pH of working solution.

Run#	GO	AuNPs	pH	Peak current (μA)
1	1	1	1	35.1525
2	1	1	-1	33.6617
3	1	-1	1	26.5955
4	1	-1	-1	33.1581
5	-1	1	1	17.5425
6	-1	1	-1	20.6133
7	-1	-1	1	18.3808
8	-1	-1	-1	18.0023
9	1.68	0	0	33.1518
10	-1.68	0	0	16.8467
11	0	1.68	0	35.7267
12	0	-1.68	0	29.4583
13	0	0	1.68	25.0261
14	0	0	-1.68	19.0157
15	0	0	0	25.5447
16	0	0	0	27.2635
17	0	0	0	25.8967
18	0	0	0	28.0733
19	0	0	0	27.8733
20	0	0	0	29.8533

After all the peak currents were attained, the results were calculated by multiple linear regression to predict a model or statistic equation as follows:

$$b = (D^T * D)^{-1} * D^T * y$$

Predicted data:

$$y' = b_0 + b_1x_1 + b_2x_2 + b_3x_3 + b_4x_1^2 + b_5x_2^2 + b_6x_3^2 + b_7x_1x_2 + b_8x_1x_3 + b_9x_2x_3$$

After using statistic, the following equation was obtained.

$$I_p = 27.21 + 6.21(\text{GO}) + 1.72(\text{AuNPs}) + 0.04(\text{pH}) - 1.02(\text{GO})^2 + 1.55(\text{AuNPs})^2 - 2.08(\text{pH})^2 + 0.94(\text{GO} \times \text{AuNPs}) - 0.31(\text{GO} \times \text{pH}) + 0.44(\text{AuNPs} \times \text{pH}); R^2 = 0.9140$$

where **GO** and **AuNPs** are the coded values of the amount of GO and the concentration of AuNPs, respectively, modified on a SPCE, **pH** is the coded value of the pH of working solution, and I_p is the resulting peak current.

The reliability of the multiple linear regression model can be assessed by the correlation coefficients (R^2). The obtained R^2 value of 0.9140 or 91.40% indicated good reliability of the results (>85%). Coefficient of each variable measures the impact of the variable on the response. The higher value of coefficient, the more impact of this variable has on the peak current. According to the equation above, the highest coefficient of GO (6.21) showed that the amount of GO had the highest impact on the signal. When the amount of GO increased, the current response also increased. A similar result could be seen on the concentration of AuNPs with the coefficient of 1.72. On the other hand, the pH of working solution had small effect on the current response due to a very low coefficient of pH (0.04). Therefore, physiological pH 7.4 was selected because this pH is commonly used in carbofuran research, easy to prepare, and stable for several weeks at 4°C. Coefficient interaction of GO-AuNPs (0.94) was high which confirmed that the major variables affecting the resulting peak current were the amount of GO and the concentration of AuNPs. This corresponds to the three-dimensional surface plots (Fig 4.8). The red area represents the high peak currents. The results showed that the highest peak current was achieved when the

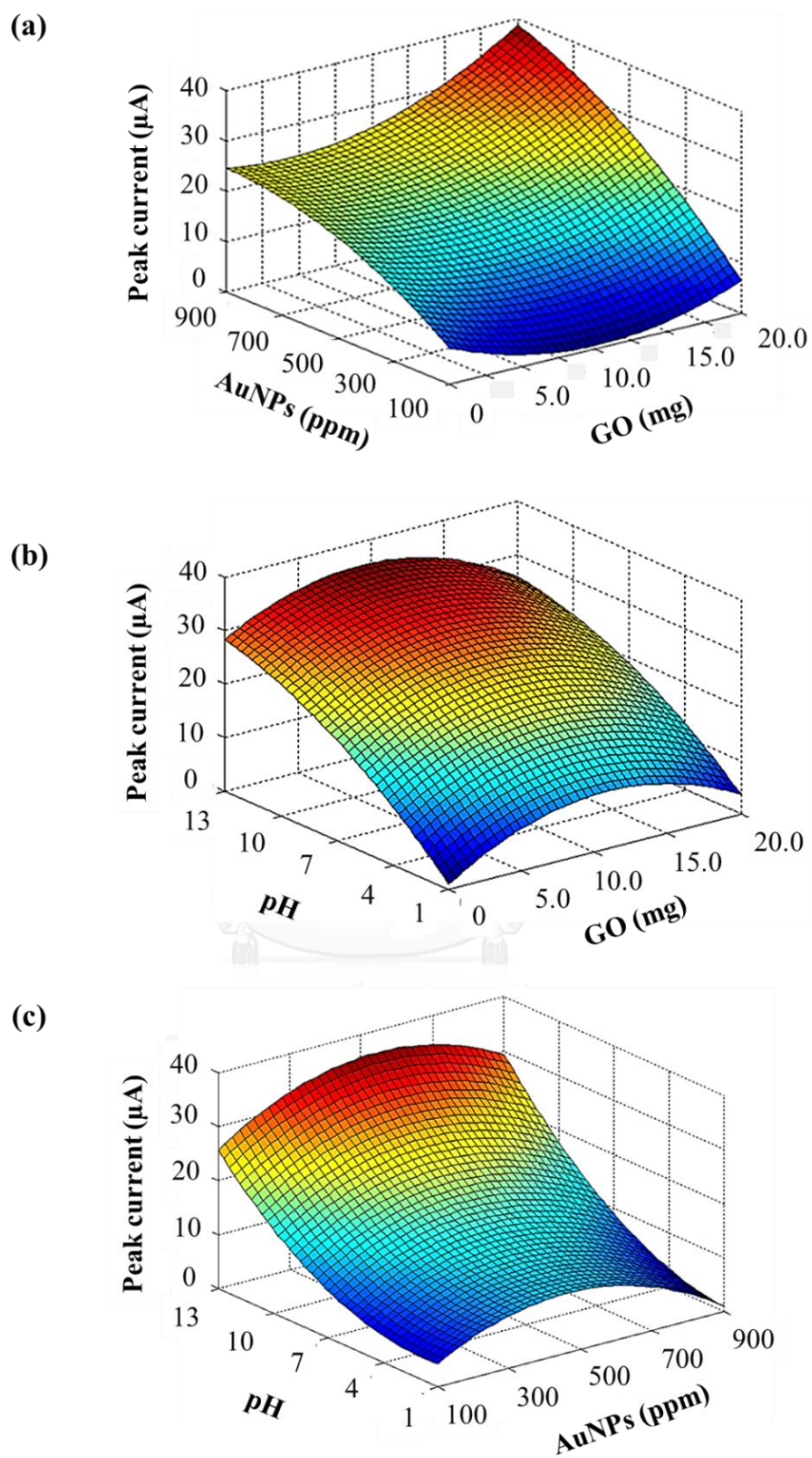


Fig. 4.8 Response surface plots showing the effects of concentration of AuNPs and amount of GO (a), pH of working solution and amount of GO (b), and pH of working solution and concentration of AuNPs (c) on the peak currents of carbofuran-phenol.

amount of GO was 18.4 mg and the concentration of AuNPs was 836 ppm. Surface plot of GO and pH was red colour covering the whole pH values indicating that pH was independent. Surface plot of AuNPs and pH was independent as well.

Due to 18.4 mg GO and 836 ppm AuNPs that provided highest response were the end of examined value, the amount of GO and AuNPs were re-optimized. The effect of amount of GO in the range of 10-80 mg per 1 g of carbon paste was studied, and the experiment using 40 mg GO provided highest response (Fig. 4.9). When the concentration of AuNPs was re-investigated it was found that the AuNPs were not stable at concentrations higher than 836 ppm. Consequently, 40 mg GO, 836 ppm AuNPs, and pH 7.4 were determined to be the optimal conditions for electrochemical determination of carbofuran-phenol at AuNPs/GO-SPCE.

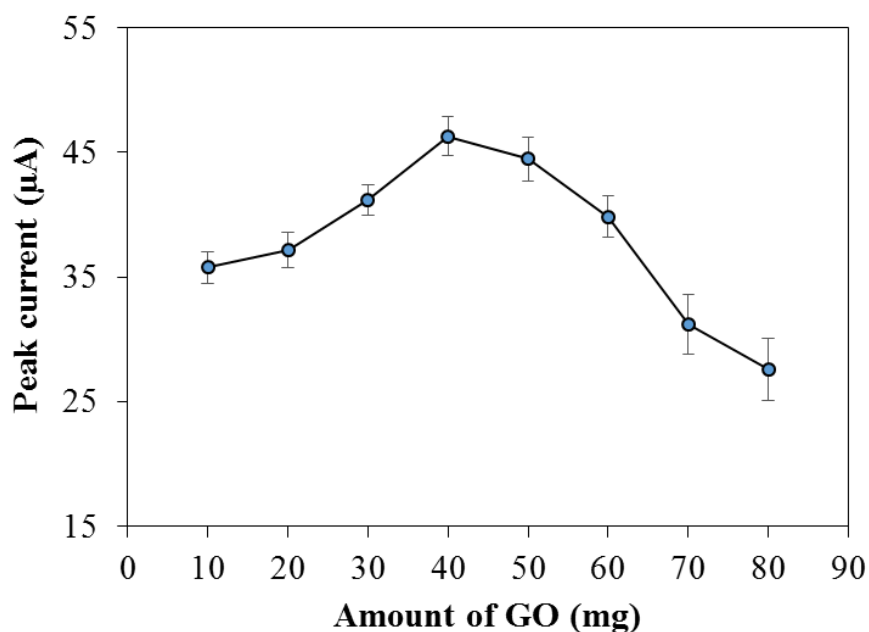


Fig. 4.9 Effect of the amount of GO on the peak current of 1.0 mM carbofuran-phenol in 0.1 M PB (pH 7.4) on AuNPs/GO-SPCE.

4.3 Electrochemical characterization of AuNPs/GO-SPCE

The electrochemical behavior of carbofuran-phenol at various electrodes including a bare SPCE, a AuNPs-SPCE, a GO-SPCE and a AuNPs/GO-SPCE were compared by CV of 2.0 mM carbofuran-phenol in 0.1 M PB (pH 7.4). The results are shown in Fig. 4.10. AuNPs-SPCE, GO-SPCE and AuNPs/GO-SPCE provided higher anodic peak currents than the bare SPCE. In particular, the peak current for the AuNPs/GO-SPCE was approximately 3x higher than the bare SPCE. This observation supported the idea that GO could improve the electron transfer of carbofuran-phenol and AuNPs could increase surface area of the electrode. It can be concluded that GO and AuNPs are promising materials that can improve the electrochemical sensitivity of electrodes for carbofuran detection.

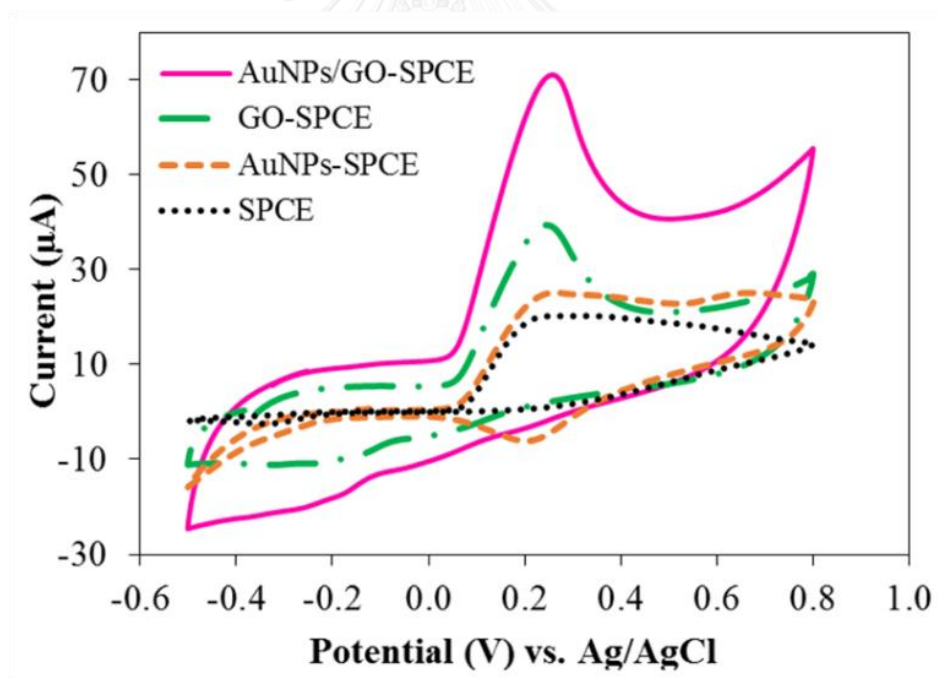


Fig. 4.10 Typical cyclic voltammograms of 2.0 mM carbofuran-phenol in 0.1 M PB (pH 7.4) on a SPCE (dotted line), a AuNPs-SPCE (dashed line), a GO-SPCE (dash-dotted line), and a AuNPs/GO-SPCE (solid line).

4.3.1 Microscopic electrode surface area

The electroactive surface area (A) of the original SPCE and AuNPs/GO-SPCE was determined by cyclic voltammetric study of a 1.0 mM $\text{Fe}(\text{CN})_6^{3-/4-}$ solution containing 0.1 M KCl at different scan rates (\mathbf{V}) according to the Randles-Sevcik equation [45].

$$I_p = 2.69 \times 10^5 A C n^{3/2} D^{1/2} \mathbf{V}^{1/2}$$

where C is the concentration of $\text{Fe}(\text{CN})_6^{3-/4-}$ (1.0 mM), n is the number of involved electrons (1 electron) and D is the diffusion coefficient of $\text{Fe}(\text{CN})_6^{3-/4-}$ ($7 \times 10^{-6} \text{ cm}^2 \text{ s}^{-1}$) [45]. As shown in Fig. 4.11, peak currents (I_p) of the SPCE and the AuNPs/GO-SPCE were plotted versus the square root of the scan rates ($\mathbf{V}^{1/2}$). The electroactive surface areas were calculated to be 0.109 cm^2 and 0.221 cm^2 for the bare SPCE (Fig. 4.11 a) and the modified electrode (Fig. 4.11 b), respectively. This can be concluded that the electroactive surface area of the developed AuNPs/GO-SPCE increased 103% compared with the unmodified electrode. This result supports the idea that graphene oxide and nanoparticles of gold can increase the surface area of electrode.



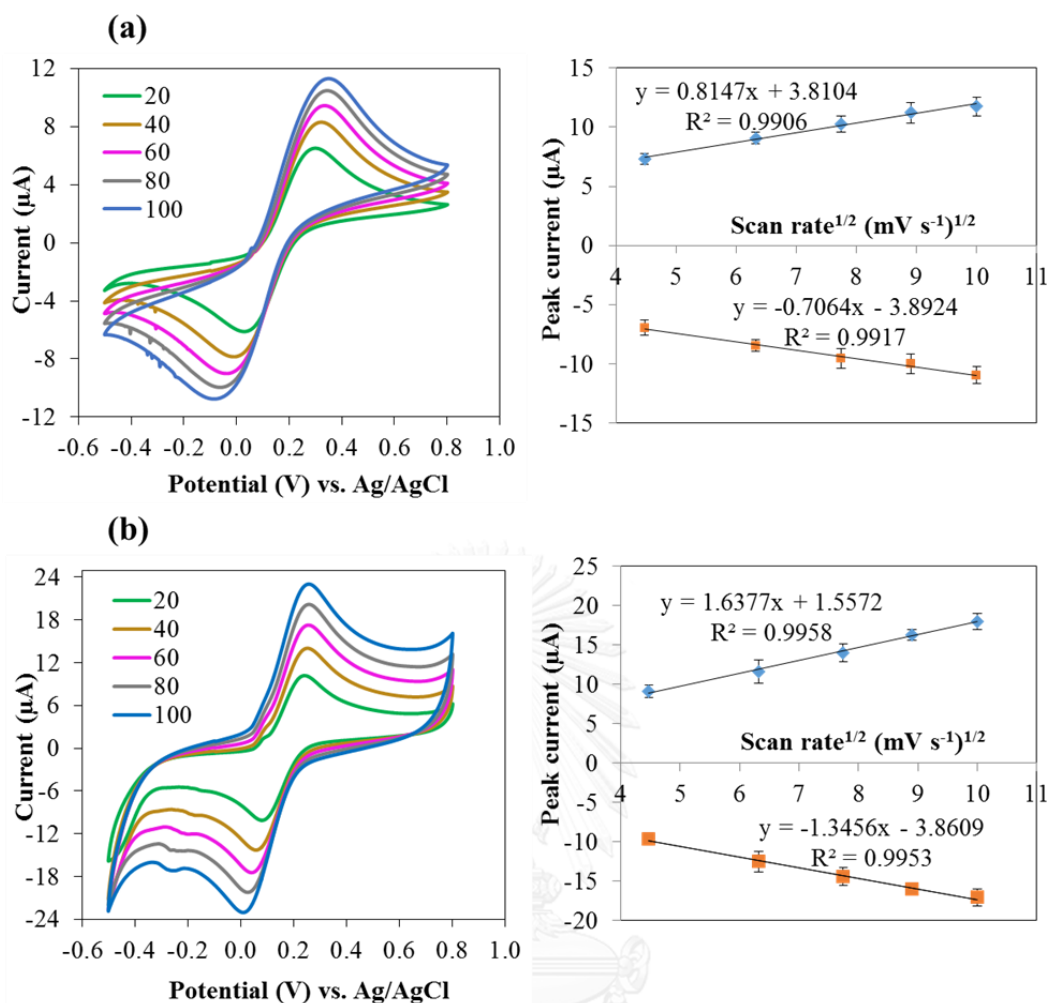


Fig. 4.11 Typical cyclic voltammograms (left) and I_p - $V^{1/2}$ plots of 1.0 mM $[\text{Fe}(\text{CN})_6]^{3-/4-}$ solution containing 0.1 M KCl on a bare SPCE (a) and a AuNPs/GO-SPCE (b) at various scan rates from 20 to 100 mV s^{-1} .

4.3.2 Study of electrochemical process of carbofuran-phenol

CV of carbofuran-phenol at various scan rates (20-100 mV s^{-1}) was used to investigate the redox process of carbofuran-phenol at AuNPs/GO-SPCE. According to Fig. 4.12 a, the peak potential (E_p) shifted to more positive value with faster scan rates. Plots of the current response and the square root of the scan rate (Fig. 4.12 b) was linear which is a characteristic of an electrochemical system where mass transport is mainly controlled by the diffusion of the electroactive species on the electrode surface. Furthermore, the $\log I_p$ and $\log \nu$ were plotted in Fig. 4.12 c. The slope of

carbofuran-phenol was found to be 0.57 which was close to the theoretically expected value of 0.5 for a purely diffusion controlled current [46]. This result supports the idea that the electro-oxidation of carbofuran-phenol was a diffusion-controlled redox process.

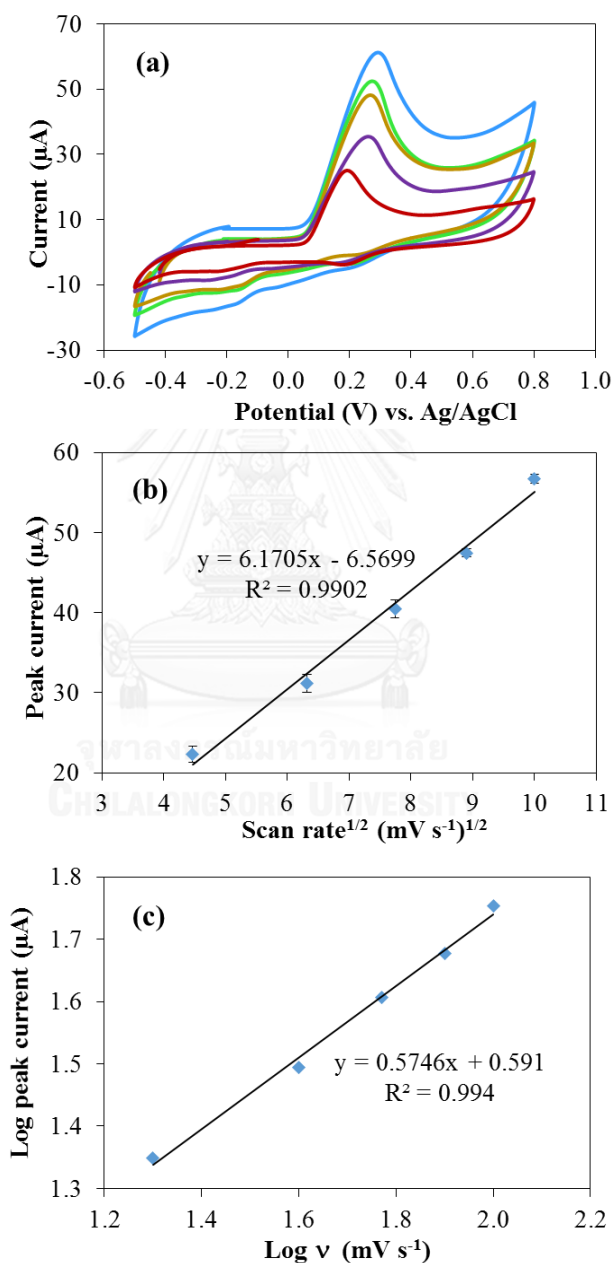


Fig. 4.12 Typical cyclic voltammograms (a), I_p - $V^{1/2}$ plot (b), and $\log I_p$ - $\log V$ plot (c) of 2.0 mM carbofuran-phenol in 0.1 M PB (pH 7.4) on AuNPs/GO-SPCE at various scan rates.

4.4 Optimization of DPV determination of carbofuran-phenol

DPV was used to improve the sensitivity of carbofuran determination. According to the literature review, the electro-oxidation of carbofuran-phenol was slow. Therefore, scan rate value was fixed at low value in this work. Scan rate can be directly calculated from the step potential divided by the interval time. As a result, a step potential and an interval time were set at a minimum value (0.01 V) and a maximum value (1 s) of Autolab PGSTAT30 potentiostats/galvanostats, respectively.

4.4.1 Effect of the supporting electrolyte

The effect of type of buffer used as a supporting electrolyte on the oxidation of carbofuran-phenol was investigated. Among various type of buffer, including acetate (dash line), borate (solid-dash line), phosphate (solid line) and Britton-Robinson buffer (dash line) (Fig. 4.13), the higher oxidation peak current of carbofuran-phenol was obtained in phosphate (6.024 μA) and Britton-Robinson (5.937 μA) buffer. However, Britton-Robinson buffer containing CH_3COOH , H_3PO_4 and H_3BO_3 requires more complicated preparation procedure than the phosphate buffer. Thus, phosphate buffer was chosen for the subsequent analytical experiments.

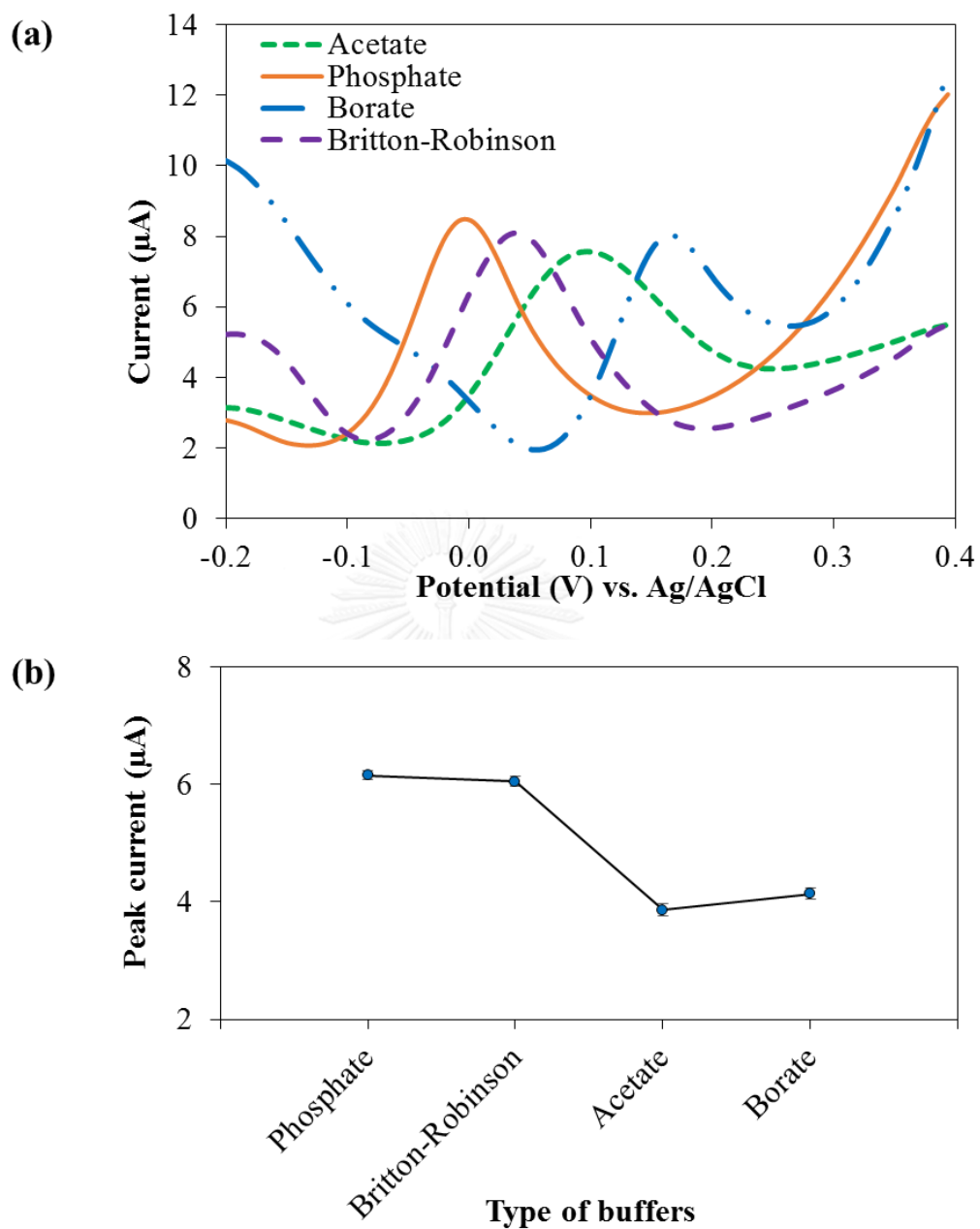


Fig. 4.13 Differential pulse voltammograms of 0.1 mM carbofuran-phenol in different type of 0.1 M buffer (pH 7.4) at AuNPs/GO-SPCE (a) and plot of peak current versus type of buffer (b).

4.4.2 Effect of the accumulation time

To achieve the sensitive detection, DPV parameters, including modulation time, modulation amplitude, accumulation potential and accumulation time, were studied. The influence of modulation time was investigated in the range of 0.1 to 0.5 V. After that, the modulation amplitude was varied from 0.01 V to 0.20 V. Finally, the effect of accumulation potential and accumulation time were examined from -0.2 to 0.2 V and 0 to 120 s, respectively. Accumulation process of carbofuran-phenol on the electrode surface is an effective approach to improve the determination sensitivity. Thus, the influence of accumulation on the anodic peak current of 0.1 mM carbofuran-phenol was optimized. The accumulation time was investigated in the range of 0 to 120 s. As shown in Fig. 4.14, the obtained peak current slowly increased when the accumulation time increased from 0 to 60 s owing to the more concentrated carbofuran-phenol on the electrode surface and did not significantly change at a longer accumulation time of 90 and 120 s because of surface saturation of the electrode. Therefore, the accumulation time of 60 s was used in subsequent analysis.

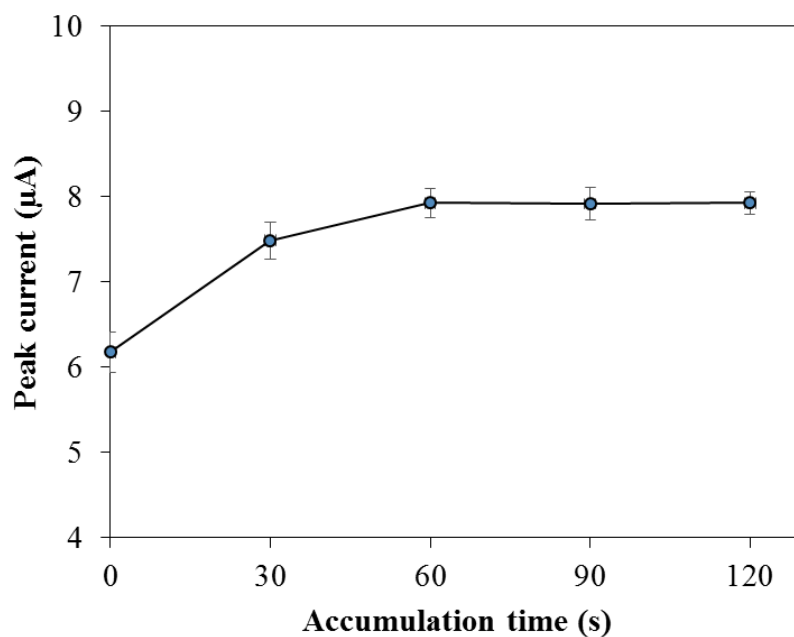


Fig. 4.14 Effect of the accumulation time on the peak current of 0.1 mM carbofuran-phenol in 0.1 M PB (pH 7.4) at AuNPs/GO-SPCE.

4.4.3 Effect of the accumulation potential

There has been reported that the accumulation potential of +0.0 V was a widely used potential for carbofuran analysis [29-31]. The dependence of current response of carbofuran-phenol on the accumulation potential was explored in the range of -0.2 to +0.2 V because the DPV peak potential of carbofuran-phenol was at around +0.0 V. The results in Fig. 4.15 show no significant difference in peak current of carbofuran-phenol at any accumulation potential and, hence, the accumulation potential did not affect the anodic peak current of carbofuran-phenol. The potential of +0.0 V was then selected for accumulation.

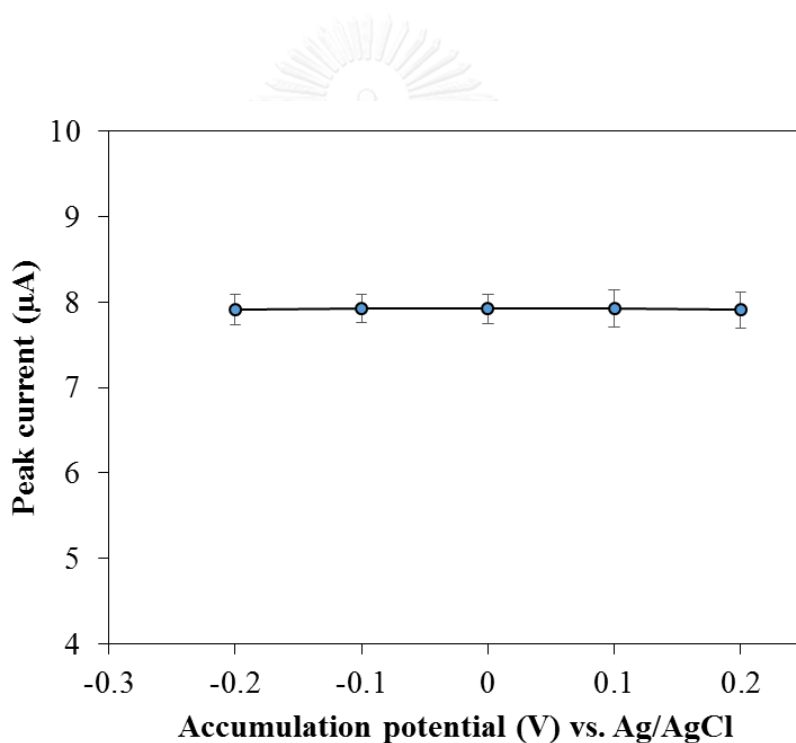


Fig. 4.15 Effect of the accumulation potential on the peak current of 0.1 mM carbofuran-phenol in 0.1 M PB (pH 7.4) at AuNPs/GO-SPCE.

4.4.4 Effect of the modulation time

Dependence of the anodic peak current on the modulation time was examined from 0.1 to 0.5 s. The results in Fig. 4.16 show that the signals of carbofuran-phenol was dramatically increased from 0.1 s to 0.3 s and after 0.3 s, signals were started to decrease. The modulation time at 0.3 s was the best condition. Hence, the following section of research used the modulation time at 0.3 s.

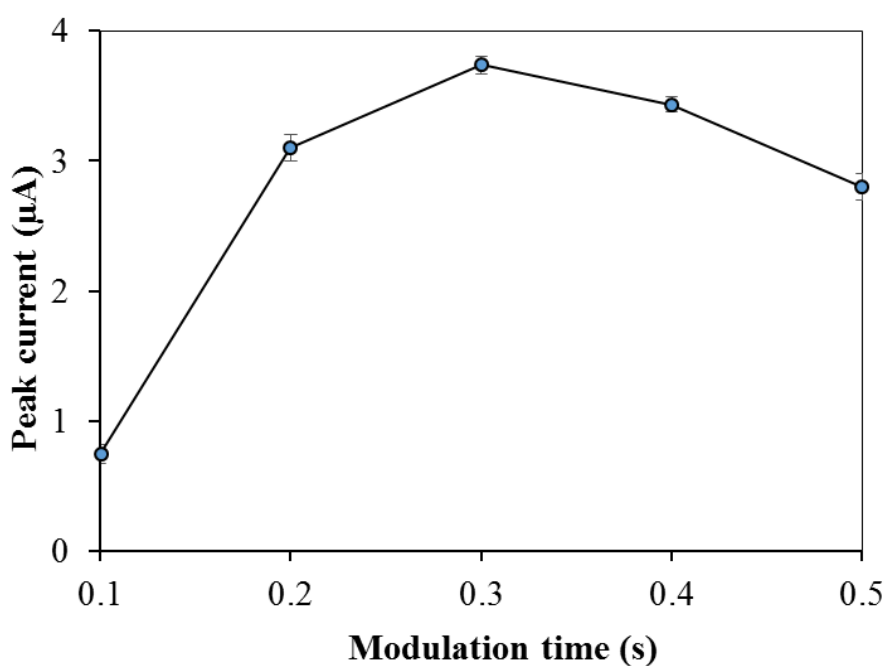


Fig. 4.16 Effect of the modulation time on the peak current of 0.1 mM carbofuran-phenol in 0.1 M PB (pH 7.4) at AuNPs/GO-SPCE.

4.4.5 Effect of the modulation amplitude

The influence of the modulation amplitude on the peak current of carbofuran-phenol is reported in Fig. 4.17. DPV amplitude was studied from 0.01 to 0.2 V, with +0.0 V as accumulation potential, accumulation time of 60 s and modulation time of 0.3 s. Larger amplitude provided a stronger current and the highest current response with small standard deviation and well-defined peak shape for carbofuran-phenol was achieved at the modulation amplitude of 0.15 V. Further increase in amplitude increased the background current as well, leading to the peak broadening. Consequently, the following section of research used the modulation amplitude at 0.15 V.

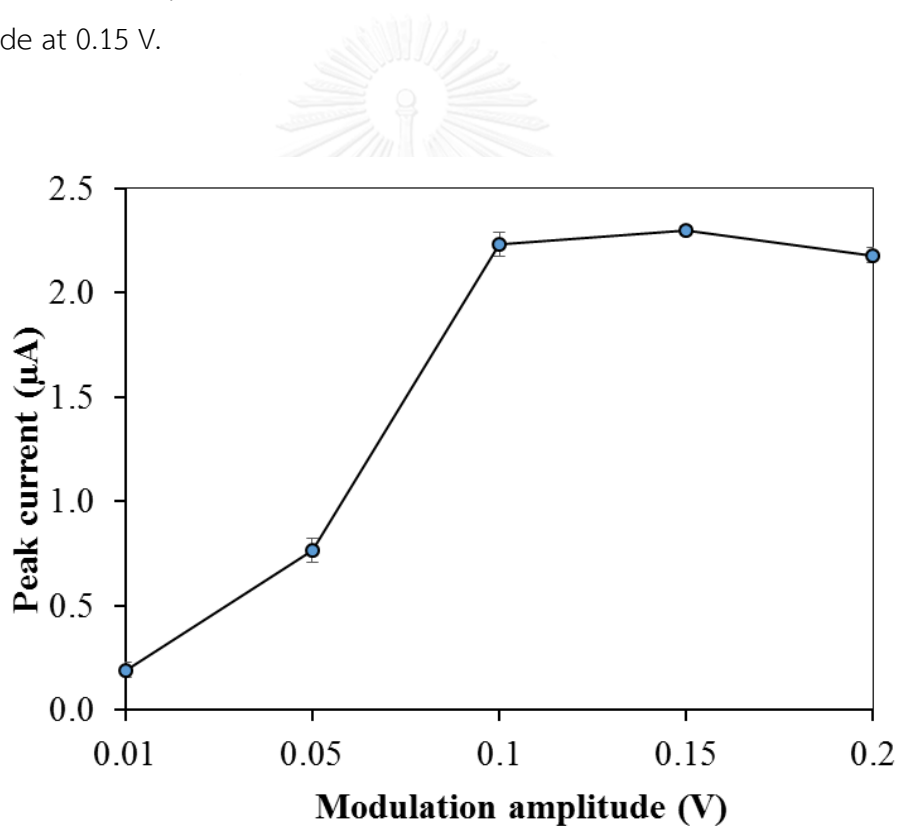


Fig. 4.17 Effect of the modulation amplitude on the peak current of 0.1 mM carbofuran-phenol in 0.1 M PB (pH 7.4) at AuNPs/GO-SPCE.

4.5 Hydrolysis of carbofuran

As previous research, carbofuran can be converted to carbofuran-phenol via hydrolysis process under temperature of 70°C within an hour in basic solution. Fig. 4.18 shows CVs of 2.0 mM carbofuran in 0.1 M PB (pH 7.4), 2.0 mM carbofuran-phenol in 0.1 M PB (pH 7.4), 0.1 M NaOH, and blank (0.1 M PB, pH 7.4). No peak was observed in both NaOH and blank indicating no interference from solution in hydrolysis process. Oxidation peak of carbofuran-phenol occurred at around 0.2 V and its peak height was obviously higher than carbofuran. It can be confirmed that hydrolysis process provided a better current response for carbofuran detection.

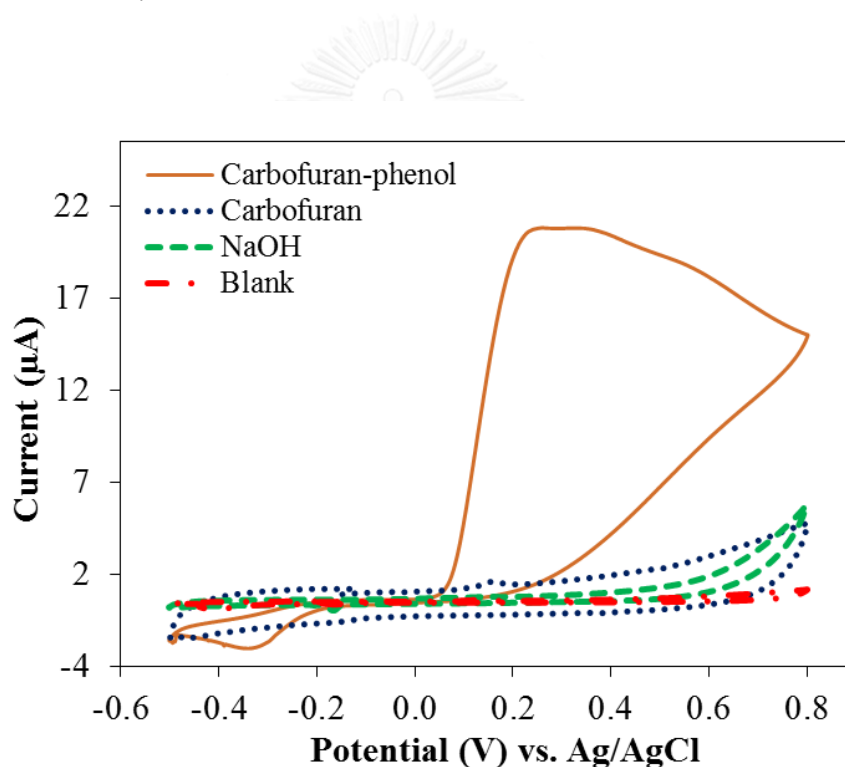


Fig. 4.18 Typical cyclic voltammograms of 2.0 mM carbofuran in 0.1 M PB (pH 7.4), 2.0 mM carbofuran-phenol in 0.1 M PB (pH 7.4), 0.1 M NaOH and blank (0.1 M PB, pH 7.4) on a AuNPs/GO-SPCE.

4.5.1 Effect of hydrolysis time, temperature and NaOH concentration

The influence of hydrolysis time (0 to 60 min) and temperature (25°C to 95°C) on the peak current was investigated by DPV of hydrolysis product of 0.1 mM carbofuran in 0.1 M PB (pH 7.4) at AuNPs/GO-SPCE. When hydrolysis time was optimized, temperature was fixed at 70°C. Meanwhile, temperature was studied, hydrolysis time was fixed at 60 min. The results in Fig. 4.19 showed that the peak current increased when hydrolysis time increased and reached the highest value at 30 min and 65°C. After that, the responses remained rather constant. Moreover, the effect of NaOH concentration was also compared between 0.1 and 0.5 M (Fig. 4.19 a). The results showed that slightly higher peak currents were obtained with 0.5 M NaOH from 0 to 30 min and after 30 min the similar results were achieved indicating that higher NaOH concentration did not increase the peak current when hydrolysis of carbofuran was complete. Therefore, hydrolysis with 0.1 M NaOH at 70°C for 40 min was chosen to ensure that carbofuran was completely hydrolyzed.

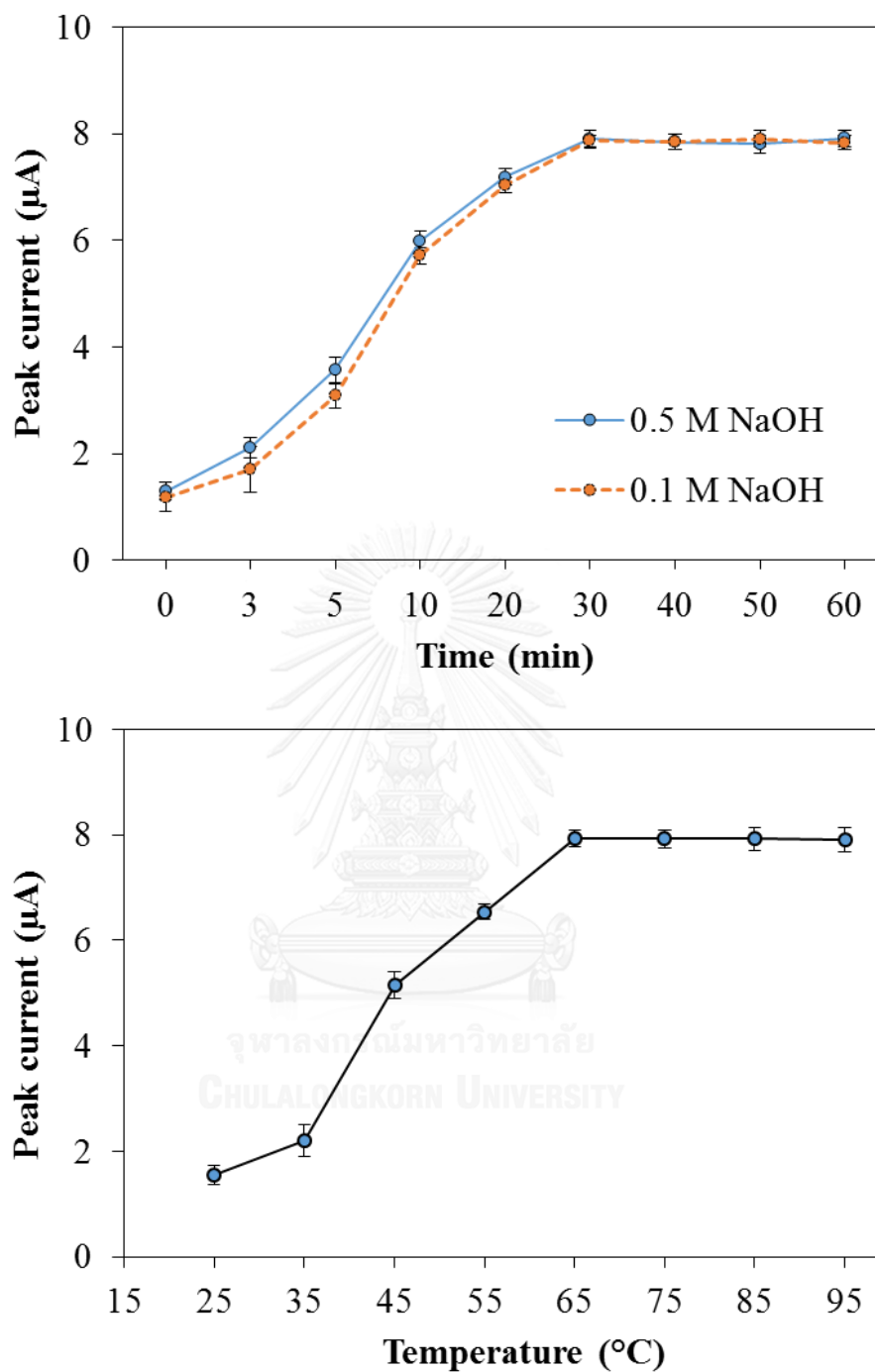


Fig. 4.19 Effect of the NaOH concentration, time and temperature for hydrolysis process on the peak current of hydrolysis product of 0.1 mM carbofuran in 0.1 M PB (pH 7.4) at AuNPs/GO-SPCE.

4.6 Analytical performance of DPV determination of carbofuran-phenol

Using the optimized conditions, DPV was carried out to determine the carbofuran-phenol in the concentration range of 1-250 μM ; the resulting voltammograms are shown in Fig. 4.20. The relationship between the carbofuran-phenol concentration and the obtained peak current was linear in the 2 concentration ranges of 1-30 and 30-250 μM with R^2 values of 0.9970 and 0.9991, respectively. The limit of detection (LOD) and the limit of quantification (LOQ) were 0.22 μM and 0.72 μM , respectively.

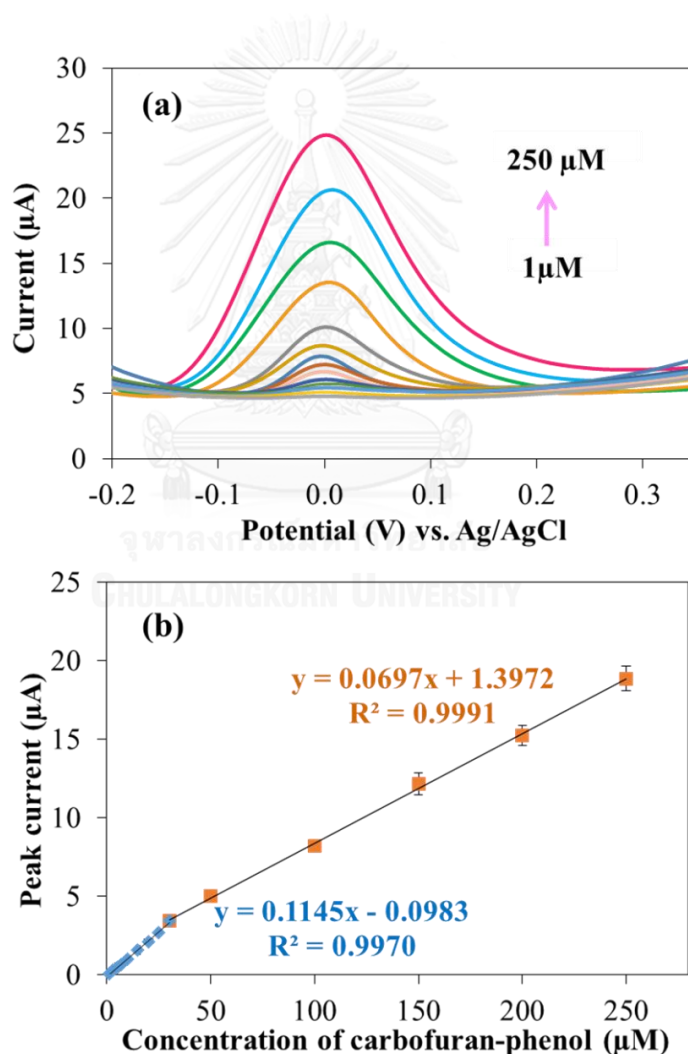


Fig. 4.20 Typical differential pulse voltammograms (a) and a standard calibration graph (b) of carbofuran-phenol in 0.1 M PB (pH 7.4) determined by DPV at a AuNPs/GO-SPCE.

4.7 Interferences study

The influence of eight other pesticides often found in agricultural products, namely chlorpyrifos, metalaxyl, carbendazim, carbaryl, propoxur, isoprocarb, methiocarb, and methomyl, on the determination of carbofuran-phenol by DPV at AuNPs/GO-SPCE were studied. The separated experiments were performed with 5 μM carbofuran-phenol in 0.1 M PB (pH 7.4) in the presence of 500 μM chlorpyrifos, 500 μM metalaxyl, 200 μM carbendazim, 5 μM carbaryl, 5 μM propoxur, 5 μM isoprocarb, 5 μM methiocarb and 180 μM methomyl. Due to no resulting DPV peaks of chlorpyrifos and metalaxyl as shown in , they did not affect the carbofuran detection. The other DPV signals are shown in Fig. 4.21. As shown in Fig. 4.22, carbendazim, a fungicide, did not interfere with carbofuran detection either, because the oxidation peak of carbendazim and carbofuran-phenol did not overlap and the interference tolerance limits was 40-fold. Some aryl carbamates, which are carbaryl and propoxur, showed peaks at the adjacent potentials with the carbofuran-phenol's peak. On the other hand, isoprocarb, methiocarb and methomyl, which are carbamate pesticides, exhibited oxidation peaks with different potentials from carbofuran-phenol's. In addition, a peak of carbofuran-phenol was higher than the peaks of isoprocarb, methiocarb and methomyl. The interference tolerance limits of isoprocarb, methiocarb and methomyl were 1-fold, 1-fold and 36-fold, respectively. These results demonstrate that the AuNPs/GO-SPCE was a highly selective sensor for carbofuran detection.

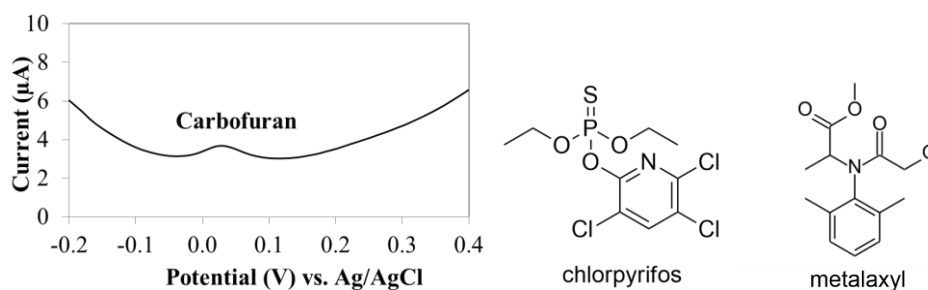


Fig. 4.21 DPV curves of 5 μM carbofuran-phenol in 0.1 M PB (pH 7.4) on AuNPs/GO-SPCE in the presence of 500 μM chlorpyrifos and metalaxyl.

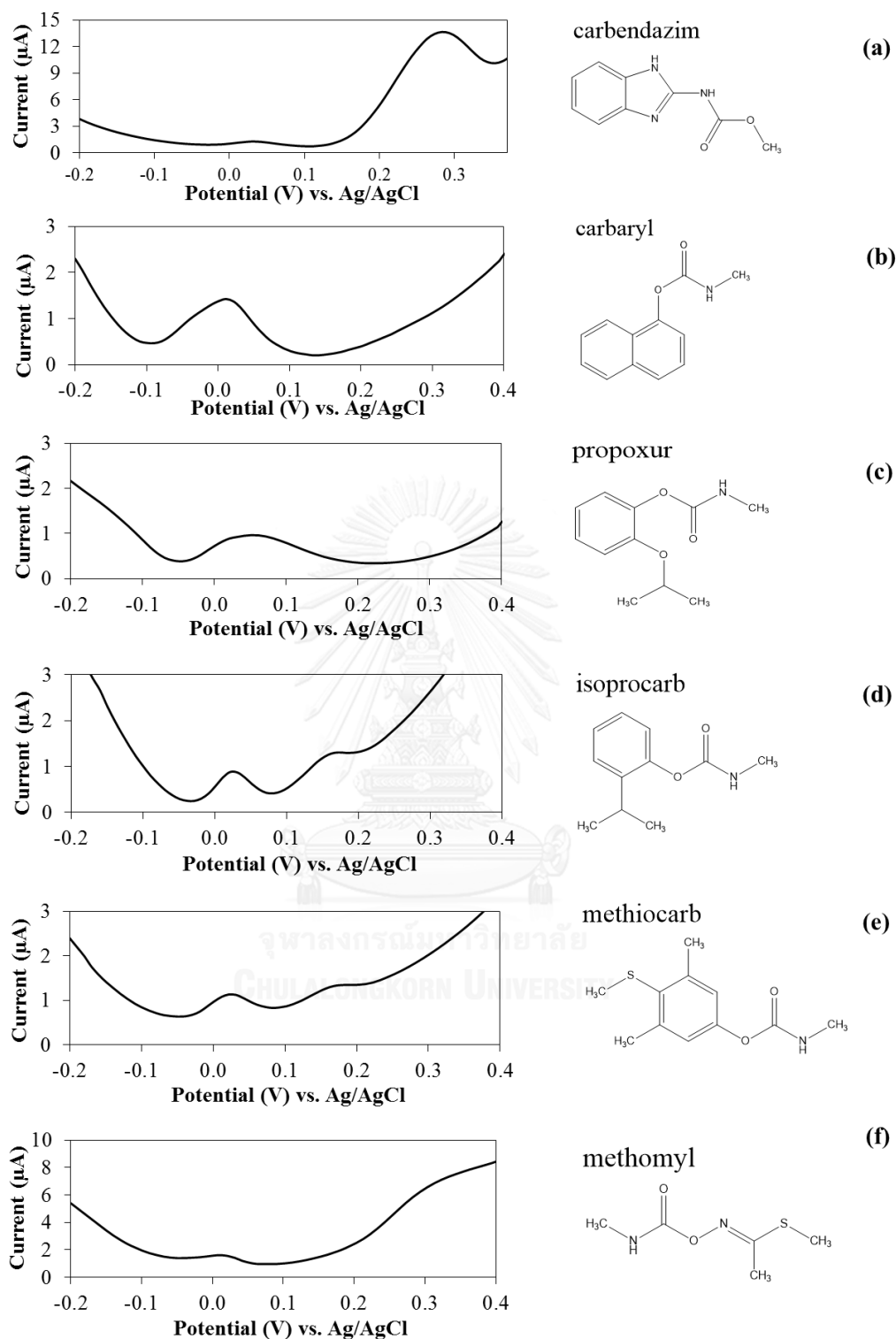


Fig. 4.22 DPV curves of 5 μM carbofuran-phenol in 0.1 M PB (pH 7.4) on AuNPs/GO-SPCE in the presence of 200 μM carbendazim (curve a), 5 μM carbaryl (curve b), 5 μM propoxur (curve c), 5 μM isoprocarb (curve d), 5 μM methiocarb (curve e), or 180 μM methomyl (curve f).

4.8 Analysis of real samples

The developed method for the determination of carbofuran by DPV at a AuNPs/GO-SPCE was applied in real cucumber and rice samples to evaluate the reliability of this method. The samples spiked with carbofuran standard at 1.106 mg/kg (5 μM in prepared sample solutions) and 6.636 mg/kg (30 μM in prepared sample solutions) were analyzed by standard addition method to avoid the matrix and the results are shown in Fig. 4.23 and Table 4.2. The detected concentrations can be obtained by direct interpolating to x-axis. The recoveries from the developed method were 92.8-107.6%. When compared to HPLC technique, the concentrations of carbofuran found by the developed method and by the conventional HPLC were not significantly different. Those indicated that the method has good accuracy.

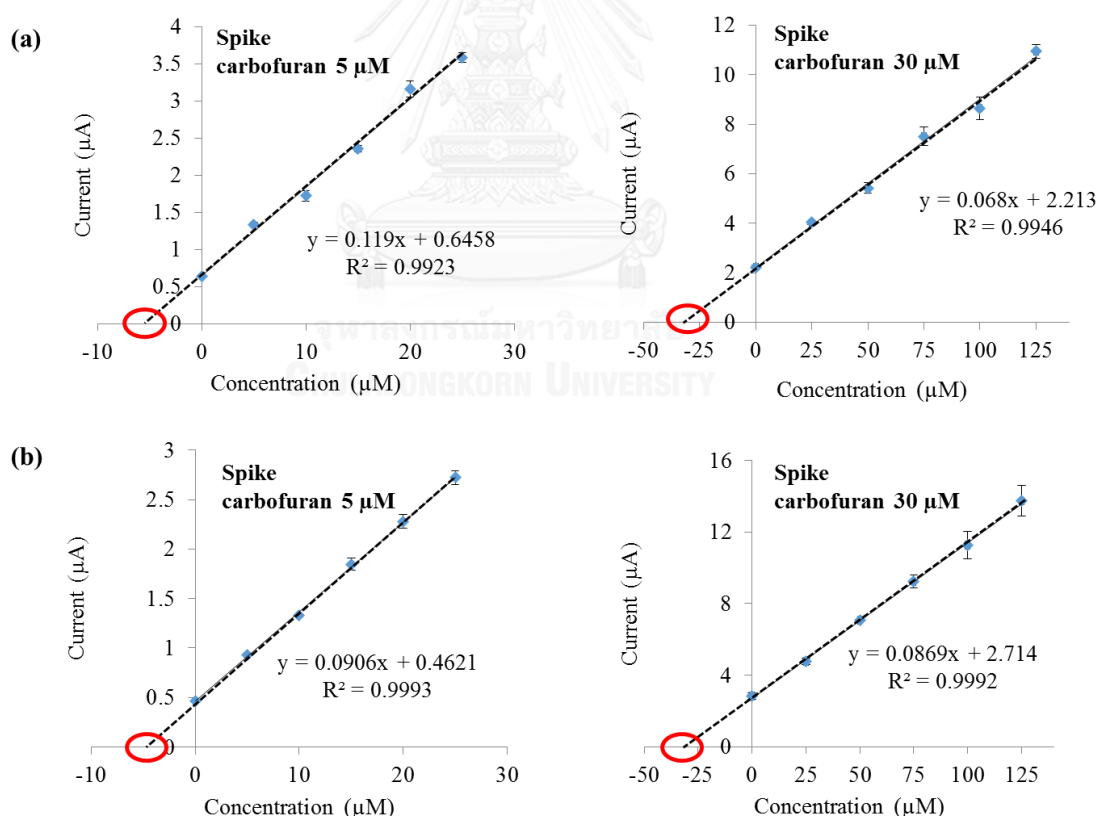


Fig. 4.23 Standard addition plots for determination of carbofuran in spiked samples of cucumber (a) and rice (b) by the developed method at a AuNPs/GO-SPCE.

Table 4.2 Determination of carbofuran concentration in spiked samples by the developed method at a AuNPs/GO-SPCE and HPLC-UV method.

Sample	Spiked (mg/kg)	DPV on AuNPs/GO-SPCE		HPLC-UV	
		Found (mg/kg)	Recovery (%)	Found (mg/kg)	Recovery (%)
Cucumber	-	Not detected	-	Not detected	-
	1.106	1.19±0.21	107.6	1.17±0.14	105.8
	6.636	6.16±0.65	92.80	6.20±0.18	93.42
Rice	-	Not detected	-	Not detected	-
	1.106	1.15±0.47	104.0	1.16±0.31	104.9
	6.636	6.95±0.82	104.7	7.12±0.46	107.3

Data are shown as the mean ± SD (N = 3) and derived from three repeats.

CHAPTER V

CONCLUSIONS

In this study, we successfully developed a novel electrochemical sensing platform with good sensitivity for carbofuran detection using inexpensive and easy fabrication screen-printed carbon electrode (SPCE) modified with graphene oxide (GO) and gold nanoparticles (AuNPs). Because of low electrochemical activity of carbofuran, it was converted to carbofuran-phenol by alkaline hydrolysis at high temperature in order to increase electrochemical response. The optimal conditions for hydrolysis were performed at 70°C for 40 min.

GO was synthesized via Hummer's method and characterized by ATR FT-IR. Then, GO was well mixed with carbon paste for screen-printing of GO-SPCE. AuNPs were synthesized by Turkevich method and characterized by UV-vis spectroscopy. Afterwards, AuNPs were modified on the working electrode by drop casting to form AuNPs/GO-SPCE. Optimal parameters of electrode modification including amount of GO, concentration of AuNPs and working solution pH examined by the central composite design (CCD) were 40 mg GO, 836 ppm AuNPs and pH 7.4, respectively. The surface of AuNPs/GO-SPCE were characterized by SEM, EDX and CV. The results showed that the AuNPs/GO-SPCE had higher surface area than a bare electrode. Moreover, the electrochemical oxidation of carbofuran-phenol on the AuNPs/GO-SPCE was shown to be diffusion-controlled process.

Differential pulse voltammetry on AuNPs/GO-SPCE was used to quantify hydrolyzed carbofuran. The effect of type of supporting electrolyte, accumulation time and potential as well as modulation time and amplitude were investigated. The optimum conditions obtained are summarized in Table 5.1.

Table 5.1 Optimization of the DPV parameters for the determination of carbofuran-phenol.

DPV parameters	Examined values	Optimal values
Type of supporting electrolyte	Acetate, borate, phosphate and Britton-Robinson buffer	Phosphate buffer
Accumulation time	0-120 s	60 s
Accumulation potential	-0.2-0.2 V	0.0 V
Modulation time	0.1-0.5 s	0.3 s
Modulation amplitude	0.01-0.2 V	0.15 V

Under the optimized conditions, the DPV method exhibited 2 linear ranges of 1-30 and 30-250 μM with R^2 values of 0.9970 and 0.9991, respectively. The limits of detection and quantitation were 0.22 and 0.72 μM , respectively. The effect of eight other pesticides which are commonly found in vegetables, namely chlorpyrifos, metalaxyl, carbendazim, carbaryl, propoxur, isoprocarb, methiocarb, and methomyl were studied. There had no significant interference in the determination of carbofuran at 100-fold excess of chlorpyrifos and metalaxyl, 40-fold excess of carbendazim, 36-fold excess of methomyl and 1-fold excess of isoprocarb and methiocarb. Furthermore, the AuNPs/GO-SPCE successfully applied to determine carbofuran concentration in cucumbers and rice by standard addition method with acceptable recoveries (92.8-107.2%). According to the above results, this sensitive and selective carbofuran detection method is very promising for simple and inexpensive analysis of agricultural samples.

Suggestion for future research

In the future, the AuNPs/GO-SPCE has effective in an application for the analysis of cucumbers and rice. The proposed detection system probably can be developed for detection carbofuran in the other samples such as soy beans, peppers, peanuts, and corns. Moreover, the AuNPs/GO-SPCE electrode can be developed for the simultaneous determination of carbendazim and methomyl because peak potential of these species are clearly separated from carbofuran and usually coexists in agricultural products.



REFERENCES

- [1] DEPARTMENT, S.A.I.S. KEY ECONOMIC INDICATORS. 2017: Thailand. 42.
- [2] COOPERATIVES, M.O.A.A. AGRICULTURAL ECONOMICS 2016. 2017: Thailand. 2.
- [3] Dai, Y., Wang, T., Hu, X., Liu, S., Zhang, M., and Wang, C. Highly sensitive microcantilever-based immunosensor for the detection of carbofuran in soil and vegetable samples. Food Chem 229 (2017): 432-438.
- [4] Otieno, P.O., Lalah, J.O., Virani, M., Jondiko, I.O., and Schramm, K.W. Carbofuran and its toxic metabolites provide forensic evidence for furadan exposure in vultures (*Gyps africanus*) in Kenya. Bull Environ Contam Toxicol 84(5) (2010): 536-44.
- [5] Li, S., Wu, X., Liu, C., Yin, G., Luo, J., and Xu, Z. Application of DNA aptamers as sensing layers for detection of carbofuran by electrogenerated chemiluminescence energy transfer. Anal Chim Acta 941 (2016): 94-100.
- [6] Vishnuganth, M.A., Remya, N., Kumar, M., and Selvaraju, N. Photocatalytic degradation of carbofuran by TiO₂-coated activated carbon: Model for kinetic, electrical energy per order and economic analysis. Journal of Environmental Management 181 (2016): 201-207.
- [7] Mansano, A.S., et al. Effects of diuron and carbofuran and their mixtures on the microalgae *Raphidocelis subcapitata*. Ecotoxicol Environ Saf 142 (2017): 312-321.
- [8] Gupta, R.C. Carbofuran toxicity. J Toxicol Environ Health 43(4) (1994): 383-418.
- [9] Extoxnet. Carbofuran. 2001.
- [10] Ruiz-Suarez, N., et al. Continued implication of the banned pesticides carbofuran and aldicarb in the poisoning of domestic and wild animals of the Canary Islands (Spain). Sci Total Environ 505 (2015): 1093-9.
- [11] Filho, A.M., dos Santos, F.N., and Pereira, P.A.d.P. Development, validation and application of a method based on DI-SPME and GC-MS for determination of pesticides of different chemical groups in surface and groundwater samples. Microchemical Journal 96(1) (2010): 139-145.
- [12] Vera-Avila, L.E., Marquez-Lira, B.P., Villanueva, M., Covarrubias, R., Zelada, G., and Thibert, V. Determination of carbofuran in surface water and biological tissue by sol-gel immunoaffinity extraction and on-line preconcentration/HPLC/UV analysis. Talanta 88 (2012): 553-60.
- [13] Xie, H.Y., et al. On-column liquid-liquid-liquid microextraction coupled with base stacking as a dual preconcentration method for capillary zone electrophoresis. J Chromatogr A 1216(15) (2009): 3353-9.
- [14] Latrous El Atrache, L., Ben Sghaier, R., Bejaoui Kefi, B., Haldys, V., Dachraoui, M., and Tortajada, J. Factorial design optimization of experimental variables in preconcentration of carbamates pesticides in water samples using solid phase extraction and liquid chromatography-electrospray-mass spectrometry determination. Talanta 117 (2013): 392-8.

- [15] Du, S., Wang, X., Sun, X., and Li, Q. Amperometric Immunosensor Based on L-Cysteine/Gold Colloidal Nanoparticles for Carbofuran Detection. Analytical Letters 45(10) (2012): 1230-1241.
- [16] Samphao, A., Suebsanoh, P., Wongsa, Y., Pekec, B., Jitchareon, J., and Kalcher, K. Alkaline Phosphatase Inhibition-Based Amperometric Biosensor for the Detection of Carbofuran. Int. J. Electrochem. Sci. 8 (2013): 3254-3264.
- [17] Jeyapragasam, T. and Saraswathi, R. Electrochemical biosensing of carbofuran based on acetylcholinesterase immobilized onto iron oxide–chitosan nanocomposite. Sensors and Actuators B: Chemical 191 (2014): 681-687.
- [18] Wang, M., Huang, J., Wang, M., Zhang, D., and Chen, J. Electrochemical nonenzymatic sensor based on CoO decorated reduced graphene oxide for the simultaneous determination of carbofuran and carbaryl in fruits and vegetables. Food Chem 151 (2014): 191-7.
- [19] Wei, H., Sun, J.J., Wang, Y.M., Li, X., and Chen, G.N. Rapid hydrolysis and electrochemical detection of trace carbofuran at a disposable heated screen-printed carbon electrode. Analyst 133(11) (2008): 1619-24.
- [20] Yang, X., Kirsch, J., Fergus, J., and Simonian, A. Modeling analysis of electrode fouling during electrolysis of phenolic compounds. Electrochimica Acta 94 (2013): 259-268.
- [21] Rao, V.K., Sharma, M.K., Pandey, P., and Sekhar, K. Comparison of different carbon ink based screen-printed electrodes towards amperometric immunosensing. World Journal of Microbiology and Biotechnology 22(11) (2006): 1135-1143.
- [22] Lin, C.-Y., Vasantha, V.S., and Ho, K.-C. Detection of nitrite using poly(3,4-ethylenedioxythiophene) modified SPCEs. Sensors and Actuators B: Chemical 140(1) (2009): 51-57.
- [23] María-Hormigos, R., Gismera, M.J., Procopio, J.R., and Sevilla, M.T. Disposable screen-printed electrode modified with bismuth–PSS composites as high sensitive sensor for cadmium and lead determination. Journal of Electroanalytical Chemistry 767 (2016): 114-122.
- [24] Sharma, M.K., Goel, A.K., Singh, L., and Rao, V.K. Immunological Biosensor for Detection of *Vibrio cholerae* O1 in Environmental Water Samples. World Journal of Microbiology and Biotechnology 22(11) (2006): 1155-1159.
- [25] Charoenkitamorn, K., Chailapakul, O., and Siangproh, W. Development of gold nanoparticles modified screen-printed carbon electrode for the analysis of thiram, disulfiram and their derivative in food using ultra-high performance liquid chromatography. Talanta 132 (2015): 416-23.
- [26] Santana, E.R., de Lima, C.A., Piovesan, J.V., and Spinelli, A. An original ferrocene oxide and gold nanoparticles-modified glassy carbon electrode for the determination of bisphenol A. Sensors and Actuators B: Chemical 240 (2017): 487-496.
- [27] Ma, M., Zhu, P., Pi, F., Ji, J., and Sun, X. A disposable molecularly imprinted electrochemical sensor based on screen-printed electrode modified with ordered mesoporous carbon and gold nanoparticles for determination of ractopamine. Journal of Electroanalytical Chemistry 775 (2016): 171-178.
- [28] Bernalte, E., Marín-Sánchez, C., Pinilla-Gil, E., and Brett, C.M.A. Characterisation of screen-printed gold and gold nanoparticle-modified carbon

- sensors by electrochemical impedance spectroscopy. Journal of Electroanalytical Chemistry 709 (2013): 70-76.
- [29] Gong, X., Bi, Y., Zhao, Y., Liu, G., and Teoh, W.Y. Graphene oxide-based electrochemical sensor: a platform for ultrasensitive detection of heavy metal ions. RSC Advances 4(47) (2014): 24653.
- [30] Wong, A., Materon, E.M., and Sotomayor, M.D.P.T. Development of a Biomimetic Sensor Modified with Hemin and Graphene Oxide for Monitoring of Carbofuran in Food. Electrochimica Acta 146 (2014): 830-837.
- [31] Suea-Ngam, A., Rattanarat, P., Wongravee, K., Chailapakul, O., and Srisa-Art, M. Droplet-based glucosamine sensor using gold nanoparticles and polyaniline-modified electrode. Talanta 158 (2016): 134-41.
- [32] Ghoreishi, S.M., Behpour, M., and Khoobi, A. Central composite rotatable design in the development of a new method for optimization, voltammetric determination and electrochemical behavior of betaxolol in the presence of acetaminophen based on a gold nanoparticle modified electrode. Analytical Methods 4(8) (2012): 2475.
- [33] Mohajeri, S., Aziz, H.A., Isa, M.H., Zahed, M.A., and Adlan, M.N. Statistical optimization of process parameters for landfill leachate treatment using electro-Fenton technique. J Hazard Mater 176(1-3) (2010): 749-58.
- [34] Wagers, K., Chui, T., and Adem, S. <pH to AuNps.pdf>. Effect of pH on the Stability of Gold Nanoparticles and Their Application for Melamine Detection in Infant Formula 7(8) (2014): 15-20.
- [35] Skoog, D.A. and D.M.W.a.F.H. Fundamentals of Analytical Chemistry. New York, USA: Saunders College Publishers, 1996.
- [36] Goldsmith, J.G. Modern Analytical Chemistry, 1st Edition (Harvey, David). Journal of Chemical Education 77(6) (2000): 705.
- [37] Nasrollahzadeh, M., Babaei, F., Fakhri, P., and Jaleh, B. Synthesis, characterization, structural, optical properties and catalytic activity of reduced graphene oxide/copper nanocomposites. RSC Advances 5(14) (2015): 10782-10789.
- [38] Tran, T.M., Ambrosi, A., and Pumera, M. Phenols as probes of chemical composition of graphene oxide. Phys Chem Chem Phys 18(44) (2016): 30515-30519.
- [39] Anand, K., Shrivastava, R., Tamilmannan, K., and Sathiya, P. A Comparative Study of Artificial Neural Network and Response Surface Methodology for Optimization of Friction Welding of Incoloy 800 H. Acta Metallurgica Sinica (English Letters) 28(7) (2015): 892-902.
- [40] Rao, T.N., Loo, B.H., B. V. Sarada, Terashima, C., and Fujishima, A. Electrochemical Detection of Carbamate Pesticides at Conductive Diamond Electrodes. Analytical Chemistry 74 (2002): 1578-1583.
- [41] HUMMERS, W.S. and RICHARD, E.O. Preparation of Graphitic Oxide. 1967.
- [42] Kimling, J., Maier, M., Okenve, B., Kotaidis, V., Ballot, H., and Plech, A. Turkevich Method for Gold Nanoparticle Synthesis Revisited. the Journal of Physical Chemistry B 110(32) (2006): 15700-15707.
- [43] Su, S., Chen, B., He, M., and Hu, B. Graphene oxide-silica composite coating hollow fiber solid phase microextraction online coupled with inductively

- coupled plasma mass spectrometry for the determination of trace heavy metals in environmental water samples. Talanta 123 (2014): 1-9.
- [44] Link, S. and El-Sayed, M.A. Size and Temperature Dependence of the Plasmon Absorption of Colloidal Gold Nanoparticles. J. Phys. Chem. B 103 (1999): 4212-4217.
- [45] Suea-Ngam, A., Rattanarat, P., Chailapakul, O., and Srisa-Art, M. Electrochemical droplet-based microfluidics using chip-based carbon paste electrodes for high-throughput analysis in pharmaceutical applications. Anal Chim Acta 883 (2015): 45-54.
- [46] Jampasa, S., Siangproh, W., Duangmal, K., and Chailapakul, O. Electrochemically reduced graphene oxide-modified screen-printed carbon electrodes for a simple and highly sensitive electrochemical detection of synthetic colorants in beverages. Talanta 160 (2016): 113-24.





APPENDIX

จุฬาลงกรณ์มหาวิทยาลัย
CHULALONGKORN UNIVERSITY

VITA

Miss Apapond Jirasirichote was born on January 28, 1992 in Nakornpathom, Thailand. She received bachelor degree at Department of Chemistry, Faculty of Science, Chulalongkorn University, Bangkok, Thailand in 2013. Next, she accordingly becomes a Master's degree of Science (Analytical Chemistry) of academic year 2016 from Chulalongkorn University.

This work was presented in the PPC and Petromat Symposium 2017, in May 23, 2017 at Patumwan Princess Hotel, Bangkok, Thailand.

